029312-2-F

ULTRA-WIDEBAND SAR FOREST EXPERIMENT NEAR RACO, MICHIGAN: JULY 1992 DATA AND RADIATIVE TRANSFER MODEL RESULTS

M. Craig Dobson

1.0 INTRODUCTION

A P-band ultra-wideband synthetic aperture radar (SAR) operated by SRI, International conducted a pair of foliage penetration experiments over forested areas in the vicinity of Raco on the eastern end of Michigan's Upper Peninsula. During these experiments, the University of Michigan performed a number of supporting activities including: (1) fabrication, deployment and positioning of trihedral corner reflectors, (2) biometric surveys of the forest stands overflown by the SAR, and (3) in situ measurements of time dependent properties of the forest pertinent to understanding and simulating forest backscattering properties.

The activities and results obtained from the first experimental period (April 4-12, 1992) have been previously reported [1]. This report documents the activities undertaken during the second experimental period (July 22 - August 1, 1992) and the resulting measurements. These are detailed in Section 2.

The potential success of a SAR for foliage penetration is limited by two main properties of the forest scene: (1) the two-way extinction of the signal during propagation through the forest and (2) the signal-to-clutter ratio for a given target of interest relative to the magnitudes of competing backscattering mechanisms in the forest crown and at the forest floor. These issues are investigated by means of simulations using a first-order, vector radiative transfer model to estimate both the transmission characteristics of various vertical layers of the forest canopy and also to estimate the net expected backscatter from the forest as the sum of various scattering pathways [2]. The model, MIMICS, is briefly described in Section 3 along with the derivation of the input parameters for the model and discussion of the model results. MIMICS is used to simulate extinction and backscatter for each forest stand observed by the ultra-wideband SAR during both the April and July, 1992 experimental periods. The model is constrained by the measured physical and biophysical properties given in [1] and in Section 2 of this report.

In general, the model results show that total canopy extinction (sum of scattering and attenuation losses) is expected to be greater for V polarization than for H polarization. Often, extinction is also found to be significantly greater during the mid-summer period due (1) to the relatively higher dielectric constants of the canopy constituent elements (trunks, branches and leaves) and (2) to the larger foliar biomass present during the summer period. The net backscatter from the forest is predicted to be highly dependent upon forest structure: tree type, trunk height, tree density and branch architecture. HH polarized backscatter is found to be dominated at P-band by multiple scattering mechanisms involving specular scattering from the ground surface and the trunk layer. As a consequence, net HH polarized backscatter from a forest is found to be inversely related to canopy extinction. This means that while conditions of lower attenuation will favor enhanced penetration of the signal through the canopy to the range locations of emplaced point targets of interest, these conditions also tend to yield greater competing background clutter induced by a lower extinction of the ground-trunk interaction mechanisms.

Since the backscatter component resulting from various pathways which include specular interactions with the forest floor will arrive contemporaneously with the direct backscatter from the forest floor, this complicates detection of targets located on the forest using ranging techniques. The model shows VV polarized backscatter to be less

sensitive to clutter arising from these ground-trunk interaction mechanisms. For VV polarization, a significant fraction of the net backscatter is generated within the crown layer, particularly by large branches.

2.0 JULY 1992 EXPERIMENT

The period of field experimentation lasted from July 22 to August 1, 1992. During this period, a number of activities were performed in support of the ultra-wideband SAR overflights and include:

(1) point calibration targets - fabrication, deployment, orientation and removal from the forest stands,
(2) leaf area index - measurement of optical transmission properties of both the forest crown layer and of the full canopy (to ground level) for estimation of foliar densities of the crown layer and ground cover,
(3) forest dielectric properties - in situ measurements of reflection coefficient at P- and L-bands for the surface layers of the soil and for woody biomass, and
(4) moisture and temperature conditions within the forest - measure the moisture status and temperatures of the surface layers of the soil and various vegetation components.

The schedule of these activities is given in Table 1.

Table 1. Schedule of Supporting Activities During July 1992

Date	Activity Description
July 22, 1992	Site survey of forest stands and suitable clearings.
July 23, 1992	LAI measurements and biometrics.
July 24, 1992	LAI measurements and corner reflector assembly.
July 25, 1992	
July 26, 1992	Corner reflector assembly.
July 27, 1992	Complete reflector fabrication.
July 28, 1992	Deploy and position reflector arrays.
July 29, 1992	Dielectric and moisture measurements.
July 30, 1992	SAR flights, dielectric and moisture measurements.
July 31, 1992	Reorient selected reflectors prior to SAR flights, dielectric and moisture measurements.
August 1, 1992	Dismantle reflector arrays.

2.1 Point Target Emplacements

Two types of trihedral corner reflectors were deployed for the July SAR overflights: (1) the reflectors fabricated for the April 1992 overflights with four foot triangular sides and (2) new reflectors fabricated of wire mesh stretched over 8 foot square-sided wooden frames. All reflectors were deployed at locations within the forest stands and associated clearings which had been mapped and flagged at the time of the April overflights, with the exception of Stand O. The maps of reflector locations given in [1] for Stands G and Q (and their associated clearings) are valid for the July 1992 SAR experimental period. A suitable clearing in the vicinity of Stand O was identified and flagged. The reflector arrays for Stand O and its associated clearing are mapped in Figure 1.

Figure 1. Trihedral corner reflector arrays at stand 0 and the associated clearing.

a. Stand 0 - Forest

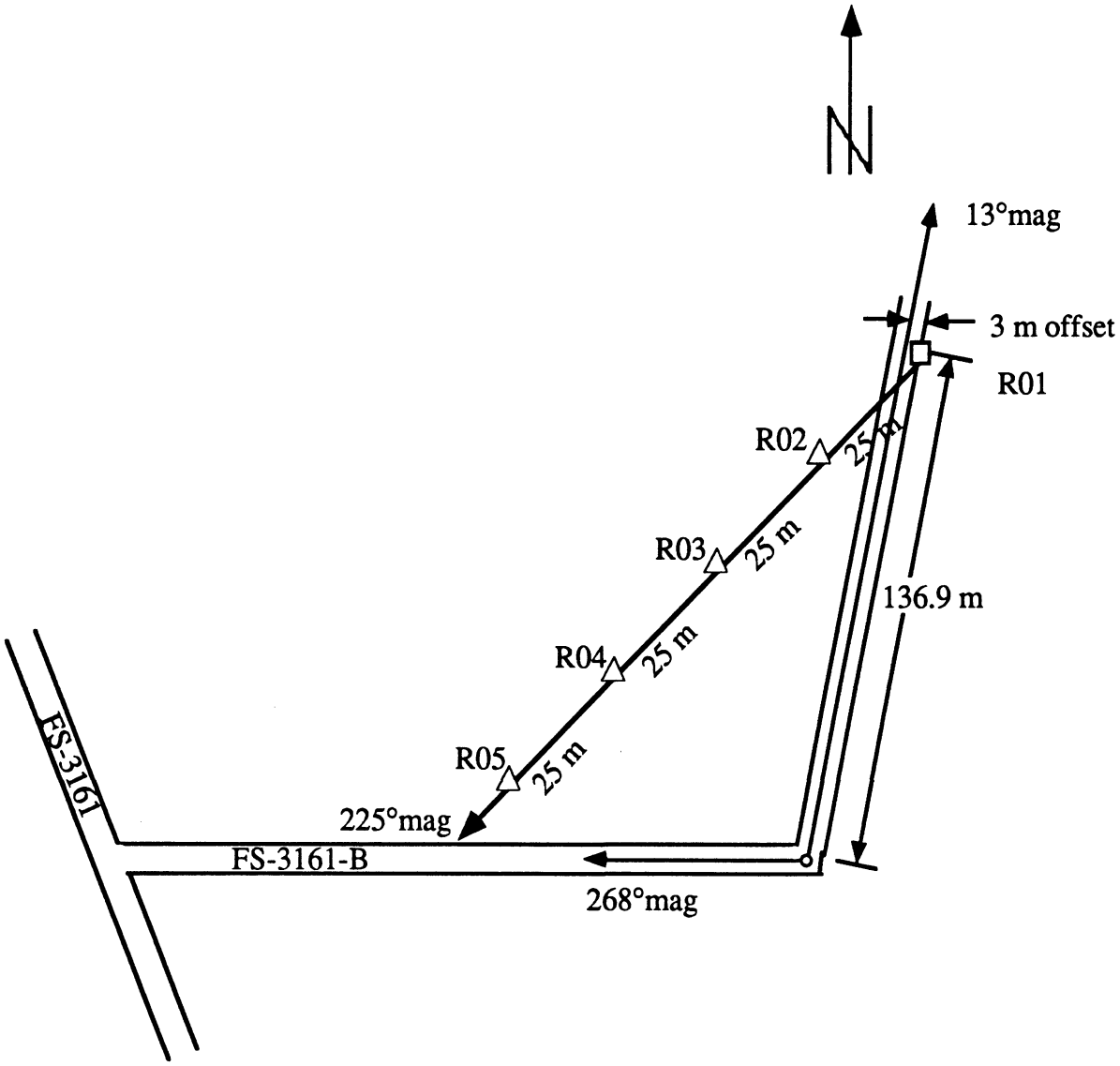

b. Clearing near stand 0 (1 mile NW of Stand 0)

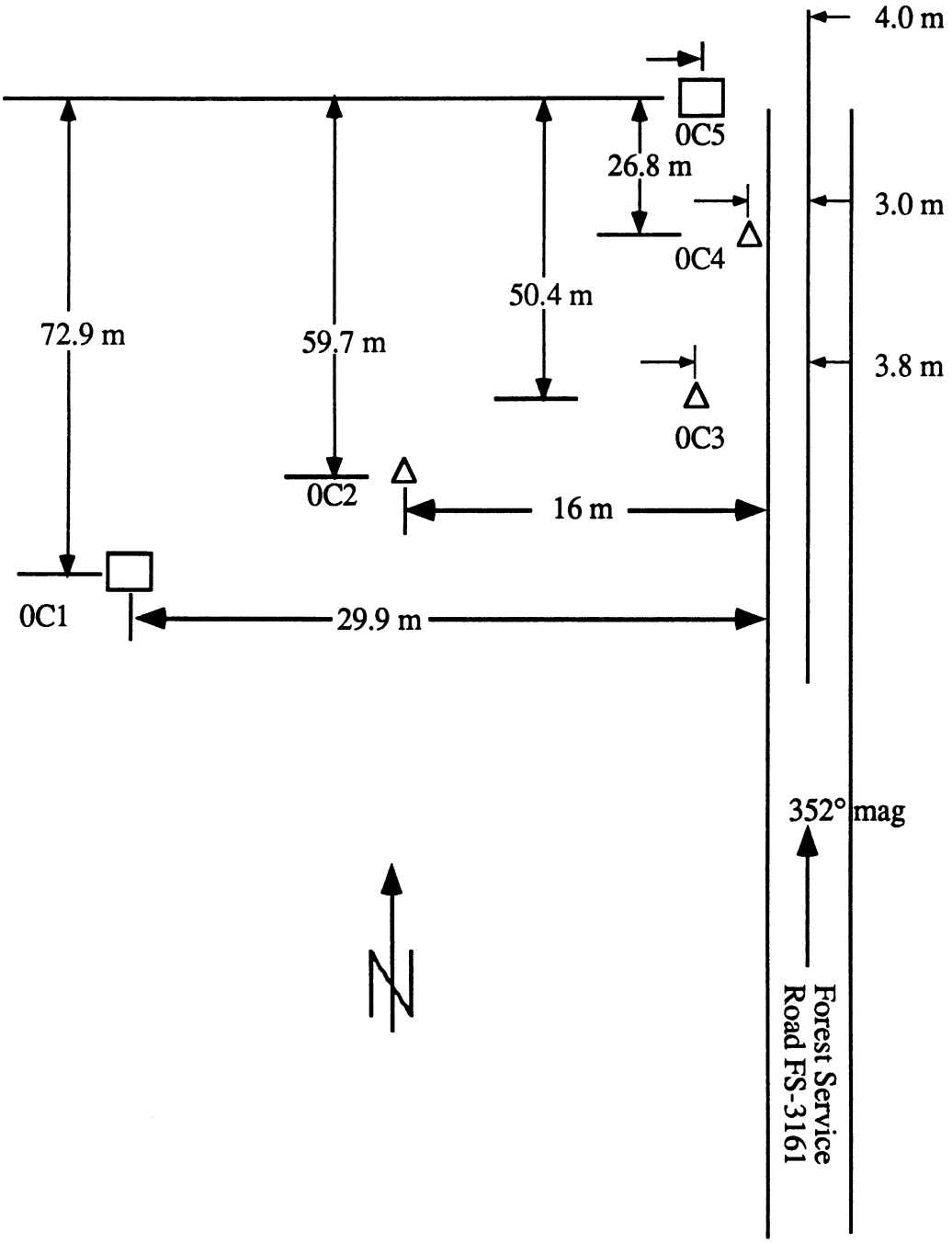

The locations of specific corner reflectors within any given forest stand or associated clearing were determined in consultation with SRI personnel. At a given stand or clearing, a transect was first surveyed using a Brunton compass and tape measures to run at an azimuth orthogonal (90°) from the magnetic heading of the expected flight line. At pre specified distances, wire surveyors flags were inserted to mark the locations for the reflectors. As needed, lateral offsets from this transect were surveyed (also using the Brunton compass and measuring tapes) to define additional reflector locations and the positions marked with wire flags. The flags were labeled to show location and target number.

The targets were transported by truck and deployed by hand at the pre specified locations. Each reflector was set in place such that the near-vertical leg at the rear of the reflector was located at the wire flag. The targets were oriented using a Brunton compass to align the front edge of the base of the trihedral to be parallel to the expected heading of the SAR and assumes the SAR to be looking to the left side. This angle is given as the azimuth angle and is accurate to +/- 1°. The tilt angle of the reflector is defined as the angle (from vertical) of the rear leg of the trihedral. Angular positioning was accomplished using vertical dowels hammered into the soil and affixed into pre-drilled holes located at the front corners of the triangular reflectors. Generally, the reflectors were inclined at 10° +/- 2°. The tilt angles were measured on the near-vertical rear leg using a digital inclinometer accurate to 0.1°. Finally, the level of the front edge of a trihedral corner reflector was adjusted using the wooden dowels. The level angle was measured using the digital inclinometer. Positive values of level indicate that the right side is high when facing into the reflector. The reflectors were generally leveled to within +/- 2°. The positioning information for the reflector arrays is given in Table 2. Reflectors were deployed within Stands G, O and Q (and their associated clearings), and initially were oriented for the primary flight lines used on the evening of July 30, 1992. A subset of the reflectors (the 8 foot reflectors) were re-oriented (180°) after the July 30 flights for use on some flight lines flown during the morning of July 31, 1992.

2.2 In-Situ Forest Measurements

A variety of measurements were made of forest physical and biophysical properties to both characterize conditions during the SAR overflights and to support modeling efforts. Biometric surveys of relatively static (over the course of a year) properties such as tree diameter, height and stocking density (by specie) were quality checked and updated as needed. Other properties, such as those related to foliar mass, temperature and moisture conditions can vary markedly with time and therefor were measured close to the SAR overflights.

Allometric equations which are empirically derived from destructive sampling of trees are used to (1) estimate the distribution of tree heights from the measured distribution of tree diameters and (2) estimate the quantities of dry biomass contained within the trunk (or stem), the branches and the foliage. Diameter to height equations are developed for each specie and forest stand using the measured data. The biomass equations for each specie have been developed by other investigators for similar forest conditions. These biomass equations depend upon tree height and diameter and they operate on a per tree basis. Summation over all trees in the stand gives estimates of the biomass per unit area (tonnes/hectare). These equations provide estimates of foliar biomass which are "time constant" in that they do not take into account year-to-year variability due to temperature conditions, pestilence and moisture availability. One

Table 2 Orientations of corner reflectors.

Stand: G-forest **Date: July 28, 1992** **Time: 12:00**

Reflector Location	Reflector Size (feet)	Azimuth (° magnetic)	Level (° from horizontal)	Tilt (° from vertical)
RG1A	8	150	NA	NA
RG2A	4	151	3.1	13.1
RG3A	4	154	2.1	10.5
RG4A	4	154	0.6	10.8
RG5A	4	156	0.7	12.0

Stand: G-clearing **Date: July 28, 1992** **Time: 13:30**

Reflector Location	Reflector Size (feet)	Azimuth (° magnetic)	Level (° from horizontal)	Tilt (° from vertical)
GC1	8	150	NA	NA
GC2	4	148	0.4	10.6
GC3	4	150	1.8	10.3
GC4	4	152.5	0.6	10.0
GC5	8	147	NA	NA

Stand: O-forest **Date: July 28, 1992** **Time: 14:30**

Reflector Location	Reflector Size (feet)	Azimuth (° magnetic)	Level (° from horizontal)	Tilt (° from vertical)
RO1	8	135	NA	NA
RO2	4	137	0.2	10.2
RO3	4	133	0.8	12.0
RO4	4	138.5	0.0	11.5
RO5	4	134	0.6	12.4

Stand: O-clearing **Date: July 28, 1992** **Time: 15:15**

Reflector Location	Reflector Size (feet)	Azimuth (° magnetic)	Level (° from horizontal)	Tilt (° from vertical)
OC1	8	134	NA	NA
OC2	4	131	1.0	10.3
OC3	4	133	0.5	9.3
OC4	4	132.5	0.6	13.2
OC5	8	225	NA	NA

Stand: Q-forest **Date: July 28, 1992** **Time: 16:55**

Reflector Location	Reflector Size (feet)	Azimuth (° magnetic)	Level (° from horizontal)	Tilt (° from vertical)
RQ1A	4	92	-0.2	10.8
RQ2A	4	92	0.4	12.7
RQ3A	4	89	0.1	10.4

Stand: Q-clearing **Date: July 28, 1992** **Time: 17:15**

Reflector Location	Reflector Size (feet)	Azimuth (° magnetic)	Level (° from horizontal)	Tilt (° from vertical)
QC1	4	89	2.0	11.1
QC2	4	89	1.3	10.5
QC3	4	91	1.3	11.1

Table 2 (continued)

Reorientation of 8' reflectors

Stand G and clearing Date: July 30, 1992 Time: 17:05

Reflector Location	Reflector Size (feet)	Azimuth (° magnetic)	Level (° from horizontal)	Tilt (° from vertical)
RG1A	8	209	NA	NA
GC1	8	209	NA	NA
GC5	8	213	NA	NA

Stand O and clearing Date: July 31, 1992 Time: 07:00

Reflector Location	Reflector Size (feet)	Azimuth (° magnetic)	Level (° from horizontal)	Tilt (° from vertical)
OC1	8	135	NA	NA
OC5	8	136	NA	NA
RO1	8	137	NA	NA

means of measuring foliar mass is via the optical transmittance of the canopy at wavelengths with strong chlorophyll absorption. These measurements were performed using a LICOR-2000 and yield estimates of leaf area index, single-sided leaf area per unit area of ground.

Good estimates of the distributions of diameter, height, stocking density and biomass (by species) are essential in parameterizing inputs to the radiative transfer model. This model also requires parameterization of the dielectric properties of all canopy constituent elements (such as the trunks, branches and foliage) and the underlying soil and snow cover (when present). The dielectric properties are either (1) measured directly at P-band using a vector-network analyzer based portable dielectric probe to measure the reflection coefficient at a coaxial probe tip terminated in the media of interest or (2) inferred from measurements of temperature and moisture for a given media using existing semi-empirical and theoretical expressions.

2.2.1 Biometric Surveys

Biometric surveys of various forest stands were conducted to statistically describe the specie composition and size distribution of the forest. A forest stand is defined as a homogeneous forested area with respect to specie mix, stocking density (number of stems per unit area), tree height and diameter. Homogeneous forest stands of at least 4 ha in size (200 m X 200 m) were selected on the basis of (1) US Forest Service airphotos and forest compartment maps for the Hiawatha National Forest, (2) P-, L- and C-band SAR imagery acquired on April 1, 1990 and June 6, 1991 by the JPL AIRSAR and (3) ground surveys by forest ecologists and foresters. Within each homogeneous stand, a baseline of 200 m length was surveyed; orthogonal to this were surveyed a series of 5 randomly located transects each 200 m in length. Eight sample locations were randomly located along each of the 5 transects, resulting in a total of 40 sample locations per stand.

Surveys of each stand were made by forest ecologists and foresters to ascertain the following: (1) tree density by specie, (2) tree diameter, (3) tree height and (4)

biomass. At each of the 40 locations, a circular sampling plot of 100 m^2 is used to inventory every upper stratum tree (height > 5 m); this results in a 10% sampling of all upper stratum trees. Each tree is identified by specie and measured for "diameter at breast height" (height = 1.3 m). A subset of all trees is measured for height. Two heights are measured: (1) the total tree height and (2) the bole height which is the height to the lowest live branch of a given tree. Linear regression is used to establish a relationship between diameter and total height for each specie. These relationships are used to estimate the height of all measured trees. A similar procedure is applied for middle stratum trees; but the measured sample represents 3% of the total population. The middle stratum is defined as stems with 1 m < height < 5 m. The cross-sectional area of the stems is calculated from the measured diameters; when summed over all trees of a given specie within the stand, this is expressed as basal area (m^2/ha).

Dry biomass is calculated on a per tree basis using allometric relationships available in the literature for a given specie. These relationships are empirically derived from destructive sampling of many different trees over a range of age, height and diameter conditions. The calculated values are typically within +/- 10% of observed. Since deciduous species shed their leaves during the winter (and had no leaves during the April overflights), estimated foliar biomass of deciduous species is ignored for estimates of total dry biomass during the winter.

The data obtained by the biometric surveys for Stands G, O, Q and T are given in Tables 3 to 6, respectively. A summary of the average heights calculated from the regression relationships based upon measured tree diameters is given in Table 7.

2.2.2 Leaf Area Index

The leaf area index (LAI) is defined as the total single-sided surface area of all the leaves within the canopy per unit area of ground. Leaf area index is useful in calculating the biomass present in the crown of a forest stand. The units of LAI are square meter per square meter.

The Li-Cor LAI-2000 (Li-Cor Inc., Lincoln, NE) device was used to estimate the LAIs of the various stands. This device was chosen because of it's portability and ease of use. The Li-Cor device, which was designed for agricultural canopies, has been shown to be an accurate estimator of both conifer and deciduous LAI [5]. The LAI-2000 is an optical instrument that estimates LAI by comparing the amount of light incident on the forest canopy to the amount of light that penetrates the canopy.

The instrument uses a fisheye lens that projects the sky image onto five light sensitive rings. Each ring is centered around a zenith angle (7°,22°,38°,52°,68°). The incident light at each of the five zenith angles is averaged over azimuth, to produce a reading. The device is meant to measure only diffuse light, not reflected or direct sunlight. Therefore, care must be taken to (1) use the instrument under diffuse illumination conditions or (2) use view restrictors, in front of the lens, to block both direct sunlight and specular scattering by the canopy [6]. Radiation with a wavelength greater than 490nm tends to be reflected by the foliage. Therefore, the device responds only to radiation of wavelength less then 490nm, so that the foliage appears black.

The LAI of a stand of trees was found by sampling at various locations within the stand. Typically, measurements are made at each of forty randomly placed locations

Table 3. Stand G Biometric Survey.

Site Name: **Raco**
Stand Name: **Stand G**
Forest Type: **Mature Pines - Red and White**

Stratum	Tree Type			Diameter (cm)			Total Height (m)		
	Acronym	Scientific Name	Common Name	Mean	Stand. Dev.	No. of Obs.	Mean	Stand. Dev.	No. of Obs.
UPPER	ABIBAL	Abies balsamea	Balsam fir	11.22	5.84	12	11.2	5.8	11
	ACERUB	Acer rubrum	Red maple	6.35	4.53	145	13.0	6.2	13
	BETPAP	Betula papyrifera	Paper birch	16.73	6.89	11	16.3	5.2	9
	PICGLA	Picea glauca	White spruce	8.62	4.92	25	9.3	5.7	12
	PICMAR	Picea mariana	Black spruce	18.20	8.06	2	18.0	4.2	2
	PINBANX	Pinus banksiana (dead)	Jack pine (dead)	21.40	0.00	1	13.0	0.0	1
	PINRES	Pinus resinosa	Red pine	14.69	10.52	77	23.3	5.5	24
	PINRESX	Pinus resinosa (dead)	Red pine (dead)	17.10	10.40	6	10.8	5.9	6
	PINSTR	Pinus strobus	Eastern white pine	24.64	9.92	106	20.7	6.6	32
	PINSTRX	Pinus strobus (dead)	Eastern white pine (dead)	16.50	5.79	21	13.6	3.5	21
	POPGRA	Populus grandidentata	Bigtooth aspen	27.10	0.00	1	23.5	0.0	1
			Stratum Average (live only)	**17.87**	**13.42**	**407**			
MIDDLE	ABIBAL	Abies balsamea	Balsam fir	2.63	1.14	20	1.9	1.8	20
	ACERUB	Acer rubrum	Red maple	1.24	0.78	337	2.1	1.0	337
	ACERUBX	Acer rubrum (dead)	Red maple (dead)	1.10	0.00	1	1.9	0.0	1
	AMESPP	Amelanchier	Serviceberry	0.63	0.26	4	1.4	0.3	4
	BETPAP	Betula papyrifera	Paper birch	0.92	0.55	15	1.3	0.7	15
	PICGLA	Picea glauca	White spruce	2.14	1.03	15	1.5	0.6	15
	PICMAR	Picea mariana	Black spruce	2.70	0.00	1	1.7	0.0	1
	PINSTR	Pinus strobus	Eastern white pine	1.30	0.51	6	1.7	0.4	6
	PINSTRX	Pinus strobus (dead)	Eastern white pine (dead)	13.30	8.77	2	1.3	0.7	2
	PRUPEN	Prunus pensylvanica	Pin cherry	1.30	0.00	1	1.8	0.0	1
	SALSPP	Salix	Willow	0.70	0.00	1	1.2	0.0	1
	VIBCAS	Viburnum cassinoides L.	Withe-rod	0.82	0.37	9	1.3	0.2	9
			Stratum Average (live only)	**1.37**	**1.28**	**412**			
			Stand Average (live only)	**9.57**	**12.58**	**819**			

Table 3 (continued)

Stand Name: Stand G
Forest Type: Mature Pines - Red and White

Common Name	Bole Height (m)			Basal Area (m^2/ha)	Stocking Density (stems/ha)	Dry Biomass (tonnes/ha)					
	Mean	Standard Deviation	Number			Total (summer)	Total (winter)	Stem	Crown	Branch	Foliage
Balsam fir	2.5	1.1	11	0.37	30	1.40	1.40	1.07	0.34	0.17	0.17
Red maple	5.2	2.7	13	1.73	363	8.56	8.27	6.88	1.68	1.39	0.29
Paper birch	7.3	3.4	9	0.7	28	4.18	3.99	3.48	0.69	0.51	0.19
White spruce	3.7	4.1	12	0.48	63	1.60	1.60	1.28	0.31	0.17	0.14
Black spruce	7.5	4.9	2	0.14	5	0.58	0.58	0.47	0.11	0.09	0.02
Jack pine (dead)				0.09	3						
Red pine	14.8	3.9	24	19.84	193	104.96	104.96	84.48	20.47	15.04	5.44
Red pine (dead)				0.45	15						
Eastern white pine	12.5	4.3	32	14.67	265	60.75	60.75	53.76	6.99	4.92	2.07
Eastern white pine (dead)				1.25	53						
Bigtooth aspen	14.0	0.0	1	0.14	3	0.80	0.79	0.69	0.11	0.10	0.01
			Stratum Total (live only)	**38.07**	**950**	**182.82**	**182.33**	**152.11**	**30.71**	**22.39**	**8.32**
Balsam fir				0.10	156						
Red maple				0.44	2633						
Red maple (dead)				0.00	8						
Serviceberry				0.00	31						
Paper birch				0.01	117						
White spruce				0.05	117						
Black spruce				0.00	8						
Eastern white pine				0.01	47						
Eastern white pine (dead)				0.26	16						
Pin cherry				0.00	8						
Willow				0.00	8						
Withe-rod				0.00	70						
			Stratum Total (live only)	**1**	**3195**						
			Stand Total (live only)	**38.68**	**4145**						

Table 4. Biometric Survey of Stand O

Site Name: Raco
Stand Name: Stand O
Forest Type: Mature Northern Hardwoods (Maple and Beech)

Stratum	Tree Type			Diameter (cm)			Total Height (m)		
	Acronym	Scientific Name	Common Name	Mean	Stand. Dev.	No. of Obs.	Mean	Stand. Dev.	No. of Obs.
Upper	ABIBAL	Abies balsamea	Balsam fir	7.74	6.27	5	8.3	3.1	3
			Balsam fir (dead)	9.80	0.00	1			
	ACEPEN	Acer pensylvanicum	Striped maple	3.90	0.00	1	5.5	0.0	1
	ACERUB	Acer rubrum	Red maple	18.52	9.49	149	15.9	7.1	43
			Red maple (dead)	17.93	7.75	7	12.3	7.6	3
	ACESAC	Acer saccharum	Sugar maple	9.82	11.48	13	6.3	1.3	4
	BETALL	Betula alleghaniensis	Yellow birch	16.22	11.57	85	15.2	6.0	29
			Yellow birch (dead)	18.94	20.16	7	12.6	8.0	7
	FAGGRA	Fagus grandifolia	American beech	16.53	15.11	104	19.2	7.4	33
			American beech (dead)	24.28	14.10	4	14.2	5.9	3
	PINSTR	Pinus strobus	Eastern white pine	11.90	0.00	1	6.0	0.0	1
			Eastern white pine (dead)	24.40	0.00	1	9.0	0.0	1
	POPTRE	Populus tremuloides	Quaking aspen	34.80	10.63	4	23.6	3.3	4
			Quaking aspen (dead)	26.50	0.00	1	21.0	0.0	1
	TSUCAN	Tsuga canadensis	Eastern hemlock	34.84	7.72	7	15.3	2.6	7
			Stratum Average (live only)	**17.50**	**12.36**	**391**			
Middle	ABIBAL	Abies balsamea	Balsam fir	2.63	1.09	174.00	1.70	0.70	174.00
			Balsam fir (dead)	2.05	0.35	2	1.3	0.3	2
	ACEPEN	Acer pensylvanicum	Striped maple	1.39	0.70	16	1.5	0.6	16
	ACERUB	Acer rubrum	Red maple	1.33	0.79	73	1.5	0.7	73
			Red maple (dead)	2.15	0.21	2	1.3	0.1	2
	ACESAC	Acer saccharum	Sugar maple	1.52	0.75	82	1.8	1.1	82
	BETALL	Betula alleghaniensis	Yellow birch	4.35	3.05	13	2.4	1.1	13
			Yellow birch (dead)	6.97	9.04	3	2.2	0.7	3
	FAGGRA	Fagus grandifolia	American beech	1.77	0.72	498	1.9	0.9	498
			American beech (dead)	2.53	2.26	8	1.8	0.9	8
	POPTRE	Populus tremuloides	Quaking aspen	1.38	1.15	4	1.2	0.2	4
			Stratum Average (live only)	**1.93**	**1.15**	**874**			
			Stand Average (live only)	**6.74**	**9.99**	**1265**			

Table 4 (continued)

Stand Name: Stand O
Forest Type: Mature Northern Hardwoods (Maple and Beech)

Common Name	Bole Height (m)			Basal Area (m^2/ha)	Stocking Density (stems/ha)	Dry Biomass (tonnes/ha)					
	Mean	Standard Deviation	Number			Total (summer)	Total (winter)	Stem	Crown	Branch	Foliage
Balsam fir	2.0	0.0	2	0.09	13	0.21	0.21	0.16	0.05	0.03	0.03
Balsam fir (dead)				0.02	3						
Striped maple	4.0	0.0	1	0.00	3	0.01	0.01	0.01	0.00	0.00	0.00
Red maple	8.5	3.1	31	12.65	373	79.27	77.94	60.84	18.43	17.11	1.33
Red maple (dead)				0.51	18						
Sugar maple	2.5	1.0	4	0.56	35	4.87	4.83	4.36	0.50	0.46	0.04
Yellow birch	8.2	3.8	20	6.60	213	40.49	39.97	28.50	11.99	11.47	0.52
Yellow birch (dead)	4.0	2.5	4	0.97	18						
American beech	7.1	3.9	28	10.20	260	67.22	66.40	52.78	14.44	13.62	0.82
American beech (dead)				0.58	10						
Eastern white pine				0.03	3	0.09	0.09	0.07	0.02	0.01	0.01
Eastern white pine (dead)				0.12	3						
Quaking aspen	13.1	1.1	4	1.02	10	7.14	7.05	6.04	1.11	1.01	0.09
Quaking aspen (dead)				0.14	3						
Eastern hemlock	4.9	2.1	6	1.74	18	6.17	6.17	4.52	1.65	1.25	0.40
Stratum Total (live only)				**32.89**	**928**	**205.46**	**202.66**	**157.28**	**48.19**	**44.96**	**3.23**
Balsam fir				0.86	1359						
Balsam fir (dead)				0.01	16						
Striped maple				0.02	125						
Red maple				0.11	572						
Red maple (dead)				0.01	16						
Sugar maple				0.13	641						
Yellow birch				0.22	100						
Yellow birch (dead)				0.19	22						
American beech				1.11	3891						
American beech (dead)				0.05	63						
Quaking aspen				0.01	31						
Stratum Total (live only)				**2.46**	**6719**						
Stand Total (live only)				**35.35**	**7647**						

Table 5. Stand Q Biometric Survey.

Site Name: Raco
Stand Name: Stand Q
Forest Type: Northern Hardwoods - Maple

Stratum	Tree Type			Diameter (cm)			Total Height (m)		
	Acronym	Scientific Name	Common Name	Mean	Stand. Dev.	No. of Obs.	Mean	Stand. Dev.	No. of Obs.
Upper	ACERUB	Acer rubrum	Red maple	14.96	0.40	245	18.5	0.8	19
	ACERUBX	Acer rubrum (dead)	Red maple (dead)	6.84	0.30	54	9.4	0.4	53
	ACESAC	Acer saccharum	Sugar maple	10.12	0.29	455	15.2	1.1	21
	ACESACX	Acer saccharum (dead)	Sugar maple (dead)	5.69	0.29	71	7.8	0.3	70
	AMESPP	Amelanchier	Serviceberry	11.45	1.95	2	17.0	1.0	2
	FAGGRA	Fagus grandifolia	American beech	6.69	0.44	23	9.1	1.3	8
	POPTRE	Populus tremuloides	Quaking aspen	23.96	3.04	11	18.4	1.2	11
	POPTREX	Populus tremuloides (dead)	Quaking aspen (dead)	22.24	4.52	5	11.1	3.1	5
			Stratum Average (live only)	**11.08**	**6.76**	**866**			
Middle	ABIBAL	Abies balsamea	Balsam fir	2.48	0.25	4	1.3	0.2	4
	ACERUB	Acer rubrum	Red maple	1.46	0.25	15	1.4	0.1	15
	ACERUBX	Acer rubrum (dead)	Red maple (dead)	4.48	0.36	5	3.1	0.6	5
	ACESAC	Acer saccharum	Sugar maple	2.03	0.13	80	2.4	0.1	80
	ACESACX	Acer saccharum (dead)	Sugar maple (dead)	3.00	0.28	23	2.7	0.2	23
	AMESPP	Amelanchier	Serviceberry	1.22	0.11	28	1.6	0.1	28
	AMESPPX	Amelanchier (dead)	Serviceberry (dead)	1.25	0.25	4	1.9	0.5	4
	FAGGRA	Fagus grandifolia	American beech	1.90	0.77	2	1.5	0.4	2
	FAGGRA	Fagus grandifolia (dead)	American beech (dead)	3.90		1	4.4		1
	POPTRE	Populus tremuloides	Quaking aspen	1.10	0.44	4	1.8	0.5	4
	POPTREX	Populus tremuloides (dead)	Quaking aspen (dead)	0.77	0.07	3	1.3	0.1	3
			Stratum Average (live only)	**2.02**	**1.25**	**169**			
			Stand Average (live only)	**9.60**	**7.05**	**1035**			

Table 5. (continued)

Stand Name: Stand Q
Forest Type: Northern Hardwoods - Maple

Common Name	Bole Height (m)			Basal Area (m^2/ha)	Stocking Density (stems/ha)	Dry Biomass (tonnes/ha)					
	Mean	Standard Deviation	Number			Total (summer)	Total (winter)	Stem	Crown	Branch	Foliage
Red maple	9.8	0.8	19	12.68	613	73.43	71.81	57.92	15.51	13.89	1.62
Red maple (dead)				0.55	135						
Sugar maple	7.1	0.9	21	12.59	1138	67.26	66.15	57.92	9.34	8.23	1.10
Sugar maple (dead)				0.53	178						
Serviceberry	14.0	0.0	2	0.05	5						
American beech	2.0	0.7	8	0.22	58	0.89	0.86	0.70	0.20	0.16	0.03
Quaking aspen	11.8	1.5	11	1.44	28	8.43	8.30	7.21	1.21	1.09	0.12
Quaking aspen (dead)				0.57	13						
Stratum Total (live only)				**26.98**	**1842**	**150.01**	**147.13**	**123.75**	**26.26**	**23.38**	**2.88**
Balsam fir				0.02	31						
Red maple				0.03	117						
Red maple (dead)				0.06	39						
Sugar maple				0.26	625						
Sugar maple (dead)				0.15	180						
Serviceberry				0.03	219						
Serviceberry (dead)				0.00	16						
American beech				0.01	31						
American beech (dead)				0.01	8						
Quaking aspen				0.00	31						
Quaking aspen (dead)				0.00	23						
Stratum Total (live only)				**0.35**	**1054**						
Stand Total (live only)				**27.33**	**2896**						

Table 6. Stand T Biometric Survey

Site Name: Raco
Stand Name: Stand T
Forest Type: Mature Aspen/Maple

Stratum	Tree Type			Diameter (cm)			Total Height (m)		
	Acronym	Scientific Name	Common Name	Mean	Stand. Dev.	No. of Obs.	Mean	Stand. Dev.	No. of Obs.
Upper	ABIBAL	Abies balsamea	Balsam fir	3.00	0.41	4	7.1	1.7	4
	ACERUB	Acer rubrum	Red maple	10.23	8.37	406	13.8	6.7	93
	ACERUBX	Acer rubrum (dead)	Red maple (dead)	18.00	4.95	2	9.5	3.5	2
	ACESAC	Acer saccharum	Sugar maple	10.72	7.70	222	11.7	5.7	25
	ACESACX	Acer saccharum (dead)	Sugar maple (dead)	14.18	15.82	4	4.0	0.0	1
	FAGGRA	Fagus grandifolia	American beech	11.97	8.73	47	12.9	4.6	12
	FAGGRAX	Fagus grandifolia (dead(	American beech (dead)	12.90	0.00	1			
	POPGRA	Populus grandidentata	Bigtooth aspen	13.25	8.02	59	11.3	5.0	13
	POPGRAX	Populus grandidentata (dead)	Bigtooth aspen (dead)	25.17	9.50	6	18.3	2.9	3
	POPTRE	Populus tremuloides	Quaking aspen	9.71	6.63	8			
	POPTREX	Populus tremuloides (dead)	Quaking aspen (dead)	8.05	0.92	2			
	PRUPEN	Prunus pensylvanica	Pin cherry	22.80	0.00	1			
	PRUSER	Prunus serotina	Black cherry	16.70	9.93	5			
			Stratum Average (live only)	**11.00**	**8.32**	**767**			
Middle	ACERUB	Acer rubrum	Red maple	1.59	2.56	240			
	ACERUBX	Acer rubrum (dead)	Red maple (dead)	2.02	3.16	28	2.6	1.2	28
	ACESAC	Acer saccharum	Sugar maple	1.58	2.84	172	1.9	1.0	172
	AMESPP	Amelanchier	Serviceberry	1.27	0.75	31	1.7	0.7	31
	AMESPPX	Amelanchier (dead)	Serviceberry (dead)	3.70	0.00	1	3.8	0.0	1
	FAGGRA	Fagus grandifolia	American beech	2.65	2.22	16	2.4	1.5	16
	PICGLA	Picea glauca	White spruce	1.09	0.23	8	1.5	0.3	8
	POPGRA	Populus grandidentata	Bigtooth aspen	1.86	1.34	35	2.2	1.3	35
	POPGRAX	Populus grandidentata (dead)	Bigtooth aspen (dead)	2.17	3.56	21	1.7	0.7	21
	PRUSER	Prunus serotina	Black cherry	1.35	0.64	2	1.2	0.1	2
	PRUSERX	Prunus serotina (dead)	Black cherry (dead)	0.80	0.00	1	1.2	0.0	1
	SORAME	Sorbus americanus	Mountain ash	0.90	0.00	1	1.0	0.0	1
			Stratum Average (live only)	**1.65**	**2.57**	**556**			
			Stand Average (live only)	**7.07**	**8.02**	**1323**			

Table 6 (continued)

Stand Name: Stand T
Forest Type: Mature Aspen/Maple

Common Name	Bole Height (m)			Basal Area (m^2/ha)	Stocking Density (stems/ha)	Dry Biomass (tonnes/ha)					
	Mean	Standard Deviation	Number			Total (summer)	Total (winter)	Stem	Crown	Branch	Foliage
Balsam fir	3.4	0.8	4	0.00	11	0.01	0.01	0.01	0.00	0.00	0.00
Red maple	7.3	4.1	62	14.29	1097	140.80	136.53	109.61	31.19	26.92	4.27
Red maple (dead)				0.13	5						
Sugar maple	6.6	3.6	11	7.58	600	45.34	44.66	38.94	6.40	5.72	0.67
Sugar maple (dead)				0.31	11						
American beech	6.2	6	7	2.01	127	12.13	11.92	9.50	2.63	2.42	0.21
American beech (dead)				0.03	3						
Bigtooth aspen	1	0	1	2.77	159	14.35	14.11	12.42	1.94	1.70	0.24
Bigtooth aspen (dead)				0.83	16						
Quaking aspen				0.21	22	0.94	0.92	0.82	0.12	0.10	0.02
Quaking aspen (dead)				0.03	5						
Pin cherry				0.10	3	0.71	0.67	0.58	0.12	0.09	0.03
Black cherry				0.35	14	2.48	2.36	2.03	0.45	0.33	0.12
			Stratum Total (live only)	**27.31**	**2033**	**216.75**	**211.19**	**173.90**	**42.85**	**37.29**	**5.56**
Red maple				1.33	2027						
Red maple (dead)				0.24	236						
Sugar maple				1.11	1453						
Serviceberry				0.04	262						
Serviceberry (dead)				0.01	8						
American beech				0.11	135						
White spruce				0.01	68						
Bigtooth aspen				0.11	296						
Bigtooth aspen (dead)				0.22	177						
Black cherry				0.00	17						
Black cherry (dead)				0.00	8						
Mountain ash				0.00	8						
			Stratum Total (live only)	**2.71**	**4266**						
			Stand Total (live only)	**30.02**	**6299**						

Table 7. **Mean heights of live upper stratum trees calculated from measured diameter distributions using regression equations developed for each specie and within each stand.**

Stand Name	Species	Mean Height (m)	Standard Deviation (m)	Number of Observations
G	Balsam fir	10.7	5.7	12
	Red maple	8.4	4.3	145
	Paper birch	17.2	4.7	11
	White spruce	7.8	4.3	25
	Red pine	24.9	4.0	77
	Eastern white pine	21.1	4.7	106
	Stand Average	15.7	8.3	376
O	Balsam fir	8.3	3.1	3
	Striped maple	5.5	0	1
	Red maple	17.4	4.6	149
	Sugar maple	9.8	11.5	13
	Yellow birch	15.1	2.7	84
	American beech	15.6	6	104
	Eastern white pine	12.0	0	1
	Trembling aspen	34.8	10.6	4
	Eastern hemlock	15.7	2.5	7
	Stand Average	16.1	5.8	366
Q	Red maple	17.2	1.3	245
	Sugar maple	12.0	4.4	455
	American beech	8.3	2.3	23
	Trembling aspen	18.4	3.1	11
	Stand Average	13.7	3.3	734
T	Red maple	11.5	5.9	406
	Sugar maple	10.9	5.3	222
	American beech	12.8	3.2	47
	Bigtooth aspen	11.9	3.8	59
	Stand Average	11.4	5.4	734

distributed along five transects; and three observations are made at each of the forty locations. The LAI of each stand is the average of all plot LAIs sampled in that stand.

Estimating the LAI of a forest stand required two LAI instruments. In order to measure the light incident upon the top of the canopy, one Li-Cor machine was left in a clearing in automatic mode, while another was used to obtain readings under the canopy. The difference of the readings from the two devices gives canopy transmittance.

Two types of readings were taken under the canopy. The first, called "full canopy" observation, is measured at ground level so as to include all understory LAI. The second, called the "crown" observation, is measured at 1m or above the shrubs, whichever is higher. The data recorded by the instrument left in the clearing is called the "sky background reference". Details of the sampling and calibration procedure are given in Wilcox and Dobson [7]. A sample of the mean values of LAI obtained at each of 40 locations in Stand Q is given in Table 8 for several sets of observations. When considered over the whole stand, the standard deviation to mean ratio is quite low, typically less than 0.1, indicating that the stands are relatively "homogeneous".

We were originally interested in LAI of the leaves in a forest canopy. However, The trunks and branches also block incident light. Therefore, we define the actual LAI of a stand, for deciduous trees, as follows:

$$LAI_{actual} = LAI_{foliated} - LAI_{defoliated} \qquad (1)$$

The foliated measurements were made during the summer or early fall and the defoliated measurements were made during the winter or early spring. For evergreen conifers, there is no way to measure a defoliated LAI. In fact, according to Gower and Norman [5], the Li-Cor device is found to underestimate the LAI of conifers due to the geometry of the needle shoots. Therefore, an estimate of the actual LAI of conifers is calculated as:

$$LAI_{actual} = C_s * LAI_{foliated} \qquad (2)$$

where C_s is a constant that depends upon the specie of conifer. Values of C_s for red and white pines are 1.50 and 1.67, respectively [5]. Correcting for woody biomass and needle-leaf shoot geometry using equations (1-2), the resultant mean values of LAI for the forest stands used by the ultra-wideband SAR experiment are given in Table 9. Note that mean LAI is nearly the same for all of the deciduous stands.

2.2.3 Moisture and Temperature

Moisture and temperature data were obtained for the soil layer and some components of woody biomass (trunks and branches) at some of the forest stands. Scattering at a boundary between two media (such as air and soil or vegetation) is proportional to the dielectric discontinuity at the interface. At microwave frequencies, the relative dielectric constant of natural media is largely controlled by moisture content and the dry density of the media, and is proportional to both. The temperature of the fluids in the media are of secondary importance (when $T > 0°C$).

The dielectric properties of the soil layer and the vegetation canopy are required as inputs to the MIMICS model. These properties can be either measured directly in situ using a portable dielectric probe operating at the frequencies of interest or they can be inferred from measurements of moisture, density and temperature characteristics of a medium of interest using empirical and semi-empirical relationships to obtain estimates

Table 8 LAI Observations of Stand Q at Raco

Transect	Location	Sept. '90	April '91	August '91		July '92
		Full Canopy	Full Canopy	Crown	Full Canopy	Full Canopy
1	1	3.57	1.04	4.87	4.66	4.62
1	2	3.55	1.05	4.89	5.52	5.05
1	3	3.42	1.06	4.52	5.12	4.97
1	4	3.55	0.92	4.32	4.58	4.48
1	5	3.52	1.04	4.45	5.09	4.76
1	6	3.44	0.89	4.24	4.44	4.22
1	7	3.54	0.89	4.48	5.46	4.68
1	8	3.4	0.9	4.32	4.59	4.73
2	1	3.36	0.98	3.79	4.58	4.01
2	2	4.06	0.77	4.11	5.41	5.12
2	3	3.45	1.01	4.02	4.6	4.33
2	4	3	1.02	3.94	4.85	4.25
2	5	3.18	1.06	4.21	4.8	4.14
2	6	3.47	0.97	4.44	4.84	4.37
2	7	3.08	0.94	3.67	3.81	4.11
2	8	4.07	0.81	4.35	4.87	4.88
3	1	3.61	0.95	3.53	4.36	
3	2	3.81	0.94	3.86	4.38	
3	3	3.63	1.03	4.48	4.61	
3	4	3.61	0.82	4.32	4.91	
3	5	3.13	0.96	4.19	5.25	
3	6	3.16	0.83	4.29	4.21	
3	7	3.27	0.81	3.9	4.82	
3	8	3.17	0.69	4.03	4.98	
4	1	3.25	1.00	4.01	4.64	4.38
4	2	3.48	0.93	4.76	4.94	4.77
4	3	3.43	0.94	4.38	4.45	4.75
4	4	3.18	0.96	4.31	4.92	4.22
4	5	3.38	1.01	4.03	4.52	4.49
4	6	3.21	0.94	3.83	4.39	4.63
4	7	3.31	0.99	4.01	4.29	4.32
4	8	3.23	0.86	4.24	4.75	4.76
5	1	3.59	1.11	4.3	4.51	4.38
5	2	3.29	0.94	3.86	4.31	4.04
5	3	3.27	0.98	3.74	4.31	4.66
5	4	3.62	1.06	4.21	4.69	4.79
5	5	3.43	1.06	3.99	4.15	4.44
5	6	3.46	1.12	3.97	4.15	3.86
5	7	3.63	1.09	4.52	4.66	4.34
5	8	3.68	1.01	4.39	4.74	4.5
MEAN:		3.44	0.96	4.19	4.68	4.50
STD DEV:		0.24	0.10	0.31	0.37	0.31

Table 9 Mean Leaf Area Index from Measurements of Forest Stands

Stand	Date	Full Canopy		Crown Layer	
		Mean	Stand. Dev.	Mean	Stand. Dev.
G	September'90			4.94	0.44
	August'91	6.40	0.44	4.69	0.47
Q	September'90			2.48	0.24
	April'91			0.00	0.10
	August'91	3.72	0.37	3.23	0.31
	July'92	3.54	0.31		
O	September'90			3.52	0.44
	August'91	3.99	0.47	3.59	0.56
	July'92	3.89	0.37		
S	September'90			1.84	0.60
	April'91			0.00	0.15
	August'91	3.36	0.62	2.21	0.52
	July'92	3.84	0.46		
T	September'90			2.60	0.33
	April'91			0.00	0.17
	August'91	3.80	0.45	3.25	0.43
	July'92	3.53	0.41		

of dielectric properties.

Moisture and temperature profiles of the soil were measured for Stands G and O on July 29 and 31, respectively. Two soil layers were observed: (1) the upper horizon of organic material and (2) the underlying mineral soil. The organic layer is typically found to be less than 5 cm in thickness. At each stand, five independent samples were obtained for each layer (if present). The soil samples were obtained using steel cores. After oven drying to equilibrium at 105°C, the sample volumes, wet and dry weights are used to calculate bulk density, gravimetric and volumetric moisture. These values and the resultant means are given in Table 10. Where present, the organic layer of humus within the stand of northern hardwoods (Stand O) is found to be wetter than that of the coniferous forest stand (Stand G); mean volumetric moisture is found to be 0.36 and 0.21 g/cm^3 for Stands O and G, respectively. The mineral soil layers of both stands are very sandy and the volumetric moisture contents were found to be nearly identical at approximately 0.15 g/cm^3. The moisture and temperature data can be used to estimate the dielectric properties of the soil using either empirical [8] or theoretical [9] models. The empirical approach is only valid for frequencies above 1 GHz however.

A small number of trees for several species (red pine and maples) were cut and measured to determine specific density and moisture contents. Subsamples of the branch and trunk sections were cut into small disks and labeled by specie. The wet mass of each piece was recorded along with its length and diameter. The samples were later dried to equilibrium mass at 70°C. The fresh volume, wet and dry masses were used to calculate the specific density as well as the gravimetric and volumetric moistures of each section. A similar procedure was used to obtain moisture and density data for foliage (needles and broadleaves). These results are summarized in Table 11 along with the air temperatures within the stands at the times of the SAR overflights. These values of moisture and density are used together with the temperature data to estimate relative dielectric constants [10] for use by MIMICS in calculations of transmissivity and radar backscatter.

2.2.4 Dielectric Properties

The microwave dielectric properties of the soil layer and the trunk fraction of selected trees of each of the dominant species were measured during the experimental period. Because of their small size and also the general inaccessibility of branches and leaves for making direct dielectric measurements, samples were obtained for determination of specific density and volumetric moisture content of branches for the common species. Dielectric properties of the branches and leaves are then calculated from moisture, density and temperature as functions of frequency using a dual-dispersion Debye model [9]. Dielectric measurements were made during the period from July 29 - 31, 1992 in conjunction with moisture measurements. This period enveloped the SAR overflights.

The dielectric measurements used a field-portable vector network analyzer [11] to measure the reflection coefficient of a coaxial line terminated in the test medium. Separate probes were used at P-band (400 MHz), L-band (1.2 GHz) and C-band (5.0 GHz). At selected tree trunks of each of the dominant species at Stands G and O, measurements were made of the radial profile of the relative dielectric constant as a function of depth into the trunk. Measurements were made at the surface of the bark layer and then in increments of several millimeters to a maximum depth of 12 cm below the surface. A low-speed drill was used to bore a hole of slightly larger diameter than the coaxial probe tip (0.25" dia.). In order to provide good contact of the probe tip with the

Table 10 Forest Soil Measurements

Site: Raco Stand G
Time: 10:30
Date: July 29, 1992

core diameter: 1.8125 in. = 4.603 cm
core area: A = 16.64 cm^2

Location	Soil Type	Soil Temp. (°C)	Core Depth (in.)	Core Depth (cm) d	Core Volume (cm^3) V=A*d	Wet Mass (g) Mw	Dry Mass (g) Md	Tare (g) Mt	H2O Mass (g) Mwa=Mw-Md	Bulk Density (g/cm^3) Bd = (Md-Mt)/V	Gravimetric Moisture (g/g) Mg = Mwa/(Md-Mt)	Volumetric Moisture (g/cm^3) Mv = Mg * Bd
RG1B	organic	11	2	5.08	84.53	71.56	53.94	29.92	17.62	0.284	0.734	0.208
RG1B	mineral	11	2	5.08	84.53	173.30	158.46	30.87	14.84	1.509	0.116	0.176
RG2B	organic	13	1.75	4.45	73.97	60.61	48.53	29.62	12.08	0.256	0.639	0.163
RG2B	mineral	13	2	5.08	84.53	169.17	153.34	29.50	15.83	1.465	0.128	0.187
RG3B	organic	13.4	1.5	3.81	63.40	75.41	56.10	29.77	19.31	0.415	0.733	0.305
RG3B	mineral	13.4	2	5.08	84.53	104.76	92.63	29.89	12.13	0.742	0.193	0.143
RG4B	organic	12.8	1.75	4.45	73.97	59.57	48.32	29.47	11.25	0.255	0.597	0.152
RG4B	mineral	12.8	2	5.08	84.53	136.20	128.00	29.64	8.20	1.164	0.083	0.097
RG5B	organic	12	1	2.54	42.27	48.21	38.84	28.72	9.37	0.239	0.926	0.222
RG5B	mineral	12	2	5.08	84.53	148.34	134.17	29.12	14.17	1.243	0.135	0.168
Average soil temperature (°C):		12.44						organic soil averages:	13.93	0.290	0.726	0.210
								mineral soil averages:	13.03	1.225	0.131	0.154

Site: Stand O
Time: 19:00
Date: July 31, 1992

core diameter: 1.8125 in. = 4.603 cm
core area: A = 16.64 cm^2
air temperature: approx. 70°F

Location	Soil Type	Notes	Core Depth (in.)	Core Depth (cm) d	Core Volume (cm^3) V=A*d	Wet Mass (g) Mw	Dry Mass (g) Md	Tare (g) Mt	H2O Mass (g) Mwa=Mw-Md	Bulk Density (g/cm^3) Bd = (Md-Mt)/V	Gravimetric Moisture (g/g) Mg = Mwa/(Md-Mt)	Volumetric Moisture (g/cm^3) Mv = Mg * Bd
RO1	note: no organic soil for RO1 or RO2											
RO1	mineral		2	5.08	84.53	170.38	156.19	29.42	14.19	1.500	0.112	0.168
RO2	mineral		2	5.08	84.53	121.86	104.45	30.37	17.41	0.876	0.235	0.206
RO2	mineral		2	5.08	84.53	153.67	142.21	30.99	11.46	1.316	0.103	0.136
RO3	organic		0.75	1.91	31.70	49.20	40.95	30.23	8.25	0.338	0.770	0.260
RO3	mineral		2	5.08	84.53	142.59	128.57	30.72	14.02	1.158	0.143	0.166
RO4	organic		1.75	4.45	73.97	69.60	42.30	30.72	27.30	0.157	2.358	0.369
RO4	mineral		2	5.08	84.53	154.50	144.88	30.46	9.62	1.354	0.084	0.114
RO5	organic		1.25	3.18	52.83	67.52	44.49	29.23	23.03	0.289	1.509	0.436
RO5	mineral		2	5.08	84.53	138.86	126.12	29.96	12.74	1.138	0.132	0.151
								organic soil averages:	19.53	0.261	1.545	0.355
								mineral soil averages:	13.24	1.223	0.135	0.157

Table 11 Summary of July '92 Vegetation Moisture Properties

Air Temperature (°C)	30-Jul-92	31-Jul-92
Maximum	23.3	4.4
Minimum	23.9	7.8

	Stand G	Stand O	Stand Q	Stand T
Air Temperature During Overflights (°C)	12.4	7.5	7.5	7.5
Tree Trunks				
Specific Density (g/cm^3)	NA*	0.600	NA*	0.600
Gravimetric Moisture (g/g)	NA*	0.480	NA*	0.480
Volumetric Moisture (g/cm^3)	NA*	0.288	NA*	0.288
Branches				
Specific Density (g/cm^3)	NA*	0.600	NA*	0.600
Gravimetric Moisture (g/g)	NA*	0.480	NA*	0.480
Volumetric Moisture (g/cm^3)	NA*	0.288	NA*	0.288
Leaves				
Specific Density (g/cm^3)	0.330	0.330	0.330	0.330
Gravimetric Moisture (g/g)	0.646	0.573	0.580	0.584
Volumetric Moisture (g/cm^3)	0.213	0.189	0.191	0.193

NA* = not available from direct field measurements, but dielectric properties were measured at P-, L- and C-bands.

medium of interest, the bottom of the bore hole was smoothed with a flat-faced drill bit prior to dielectric measurement. At each depth, the reflection coefficient was measured three times and recorded. The recorded data was post-processed to filter individual values where good surface contact with the trunk was not maintained. The resultant values were used to calculate the relative dielectric constant of the trunk and then averaged as a function of depth for each specie.

Specular scattering by the tree trunks can lead to the dominant source of backscatter from forests at long wavelengths [12]. Scattering by the trunks is dependent upon geometry (the height and diameter distributions of the trunks), the surface roughness of the bark, and the effective relative dielectric constant of the trunk. A tree trunk is a highly layered dielectric as shown in Figures 2 to 6 for white pine, red pine, american beech, red maple and sugar maple, respectively. The dry bark layer generally is characterized by a low dielectric constant, about 3, and is of variable thickness for pines and maples. The thickness of the bark layer of aspens does not vary much with the diameter, height and age of the tree. In addition, the bark can have a rough surface for some species such as red pine and the maples while it is relatively smooth (in terms of roughness) for white pine and for aspens. Inside the bark layer is a region of very moist tissue, the cambium region, which typically has a very high dielectric constant for non-frozen trees. The magnitude of the dielectric constant in the cambium zone is specie dependent. The cambium region may be only a few millimeters thick, but the high magnitude of the dielectric constant (as much as 60) means that this region is often critical in controlling trunk scattering mechanisms. Beneath the cambium zone, the dielectric constant typically decreases to a level of 10 to 30 within the moist sapwood region. Dielectric constant of wood is proportional to moisture and density. The dielectric constant typically decreases with frequency as shown in Figures 2 - 6.

Soil dielectric properties were measured at the time of moisture sampling using the dielectric probes at P-, L- and C-bands. At each soil pit, three independent samples were obtained for each layer (organic layer and mineral soil layer). The means of all measured values are given in Table 12 for Stands G and O as measured on July 29 and 31, 1992, respectively. The measured means are very close to what would be estimated from mean moisture, density and texture of the soil using a empirical dielectric model for soil [13].

Figure 2. Measured dielectric profiles of a white pine trunk.

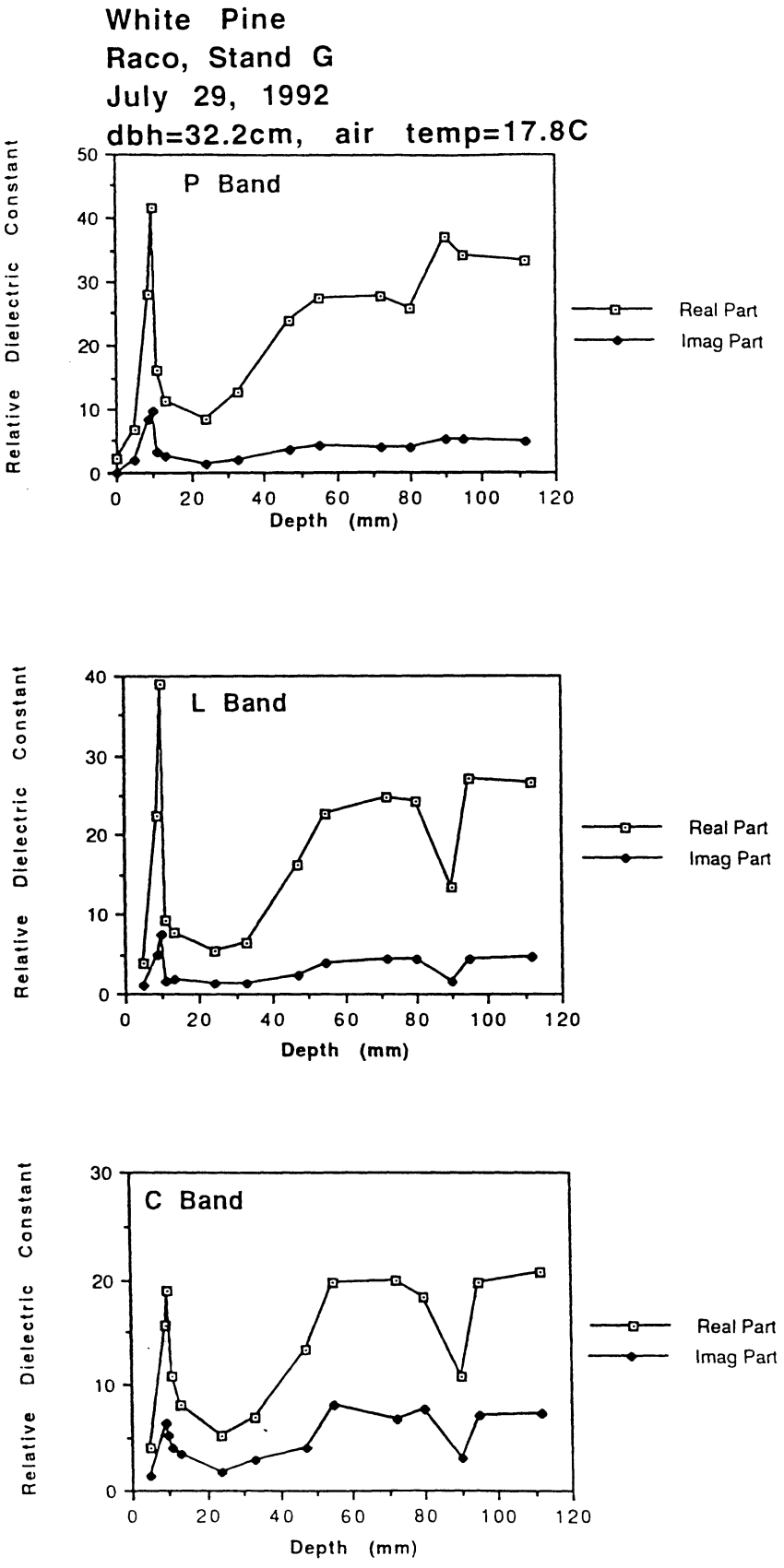

Figure 3. Measured dielectric profiles of a red pine trunk.

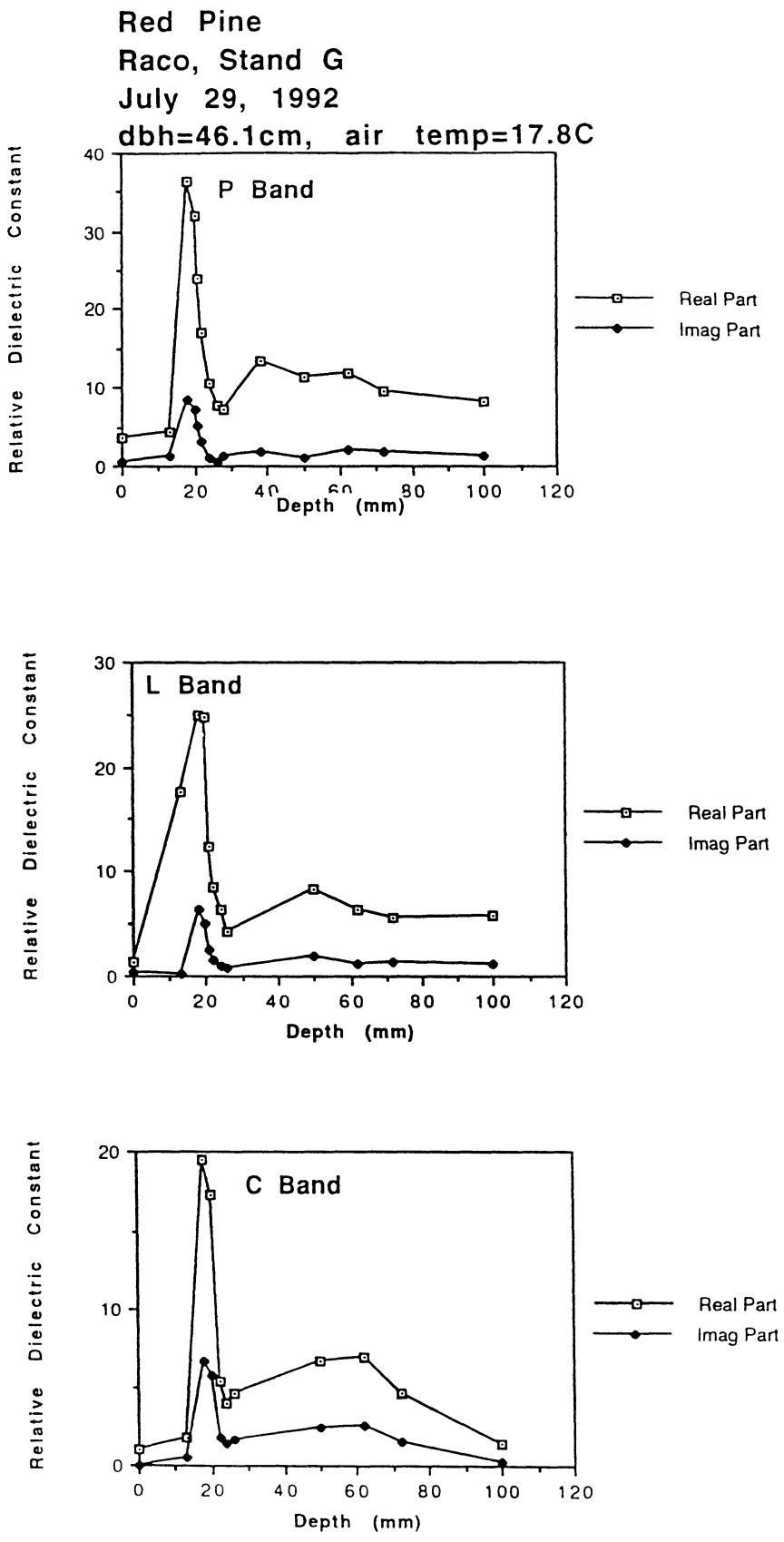

Figure 4. Measured dielectric profiles of a beech trunk.

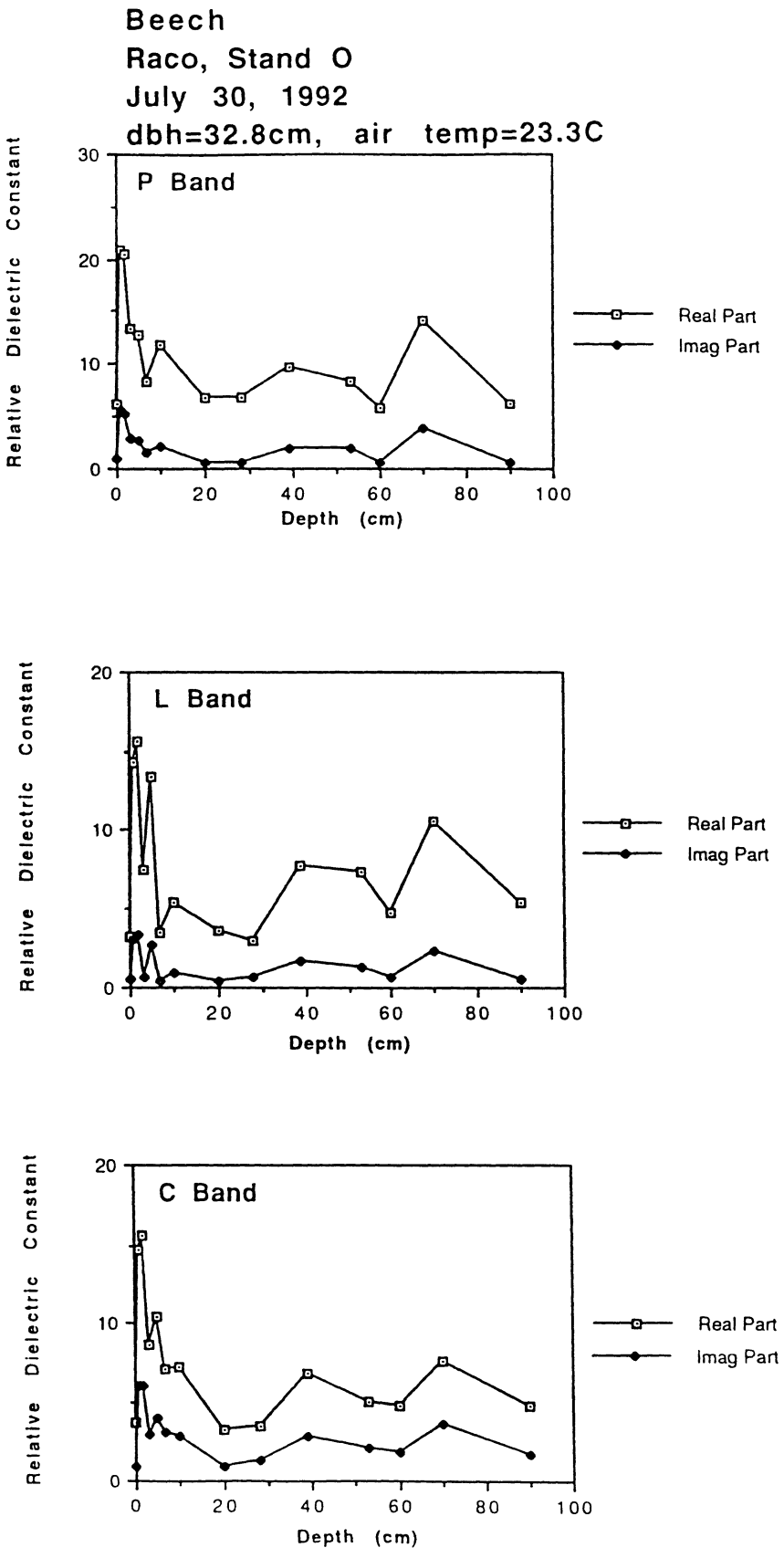

Figure 5. Measured dielectric profile of a red maple trunk.

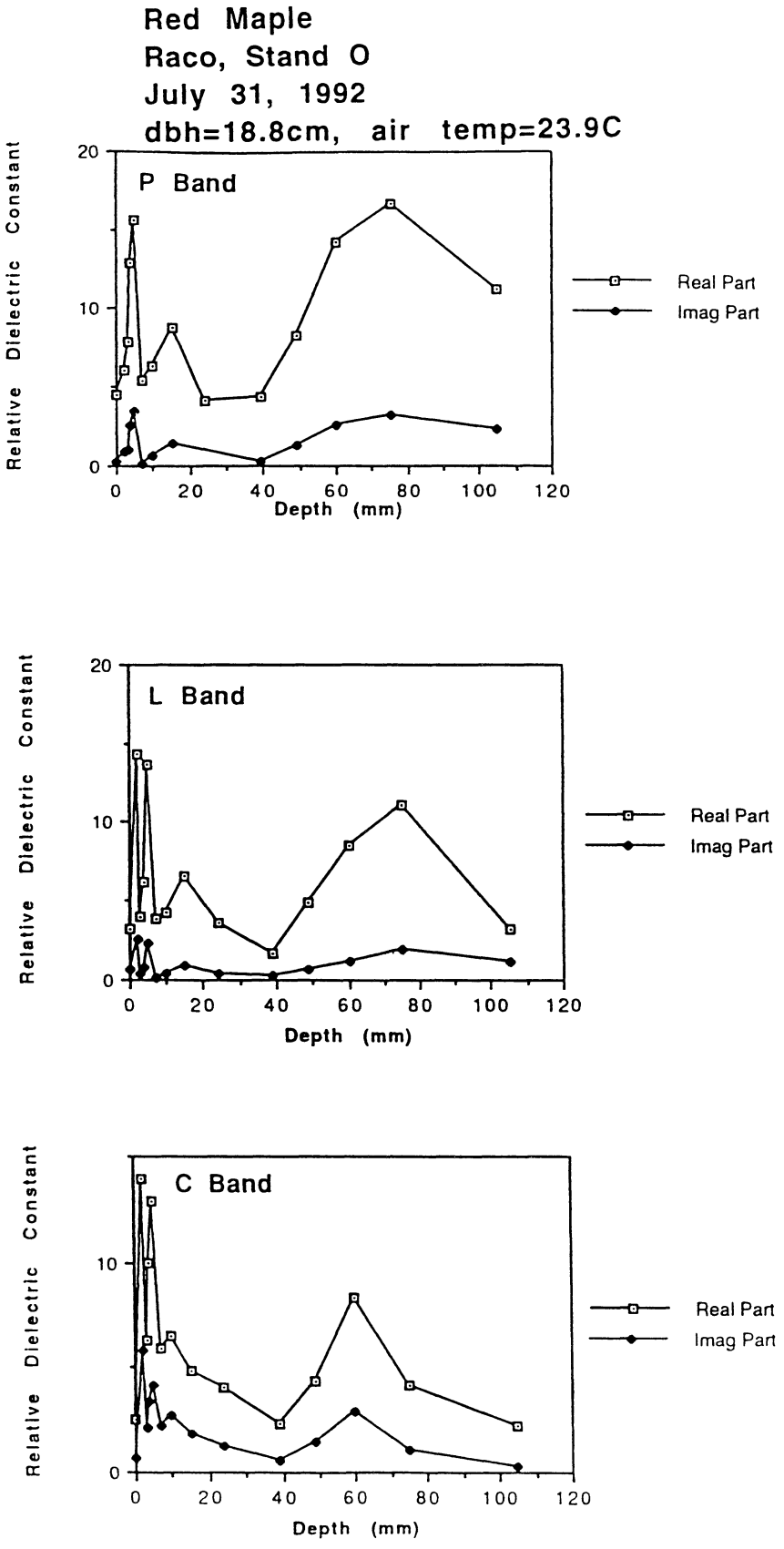

Figure 6. Measured dielectric profile of a sugar maple trunk.

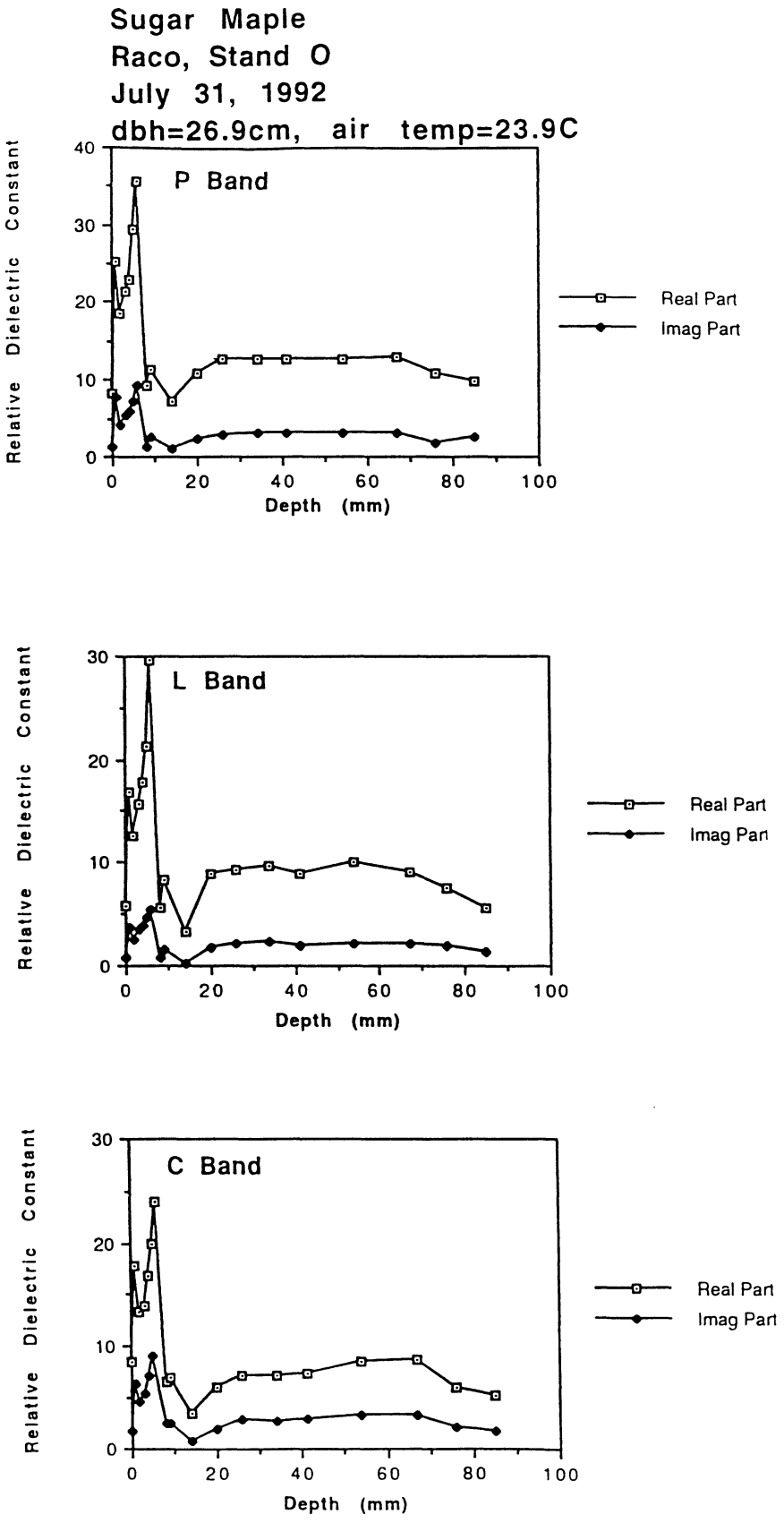

Table 12 Summary of July '92 Soil Moisture and Dielectric Properties

	Stand G	Stand O
Date	29-Jul-92	31-Jul-92
Time	10:30	19:00
Soil Temperature (°C)	12.4	NA
Bulk Density (g/cm^3)		
Organic Layer	0.290	0.261
Mineral Soil	1.225	1.223
Gravimetric Moisture (g/g)		
Organic Layer	0.726	1.545
Mineral Soil	0.131	0.135
Volumetric Moisture (g/cm^3)		
Organic Layer	0.210	0.355
Mineral Soil	0.154	0.157
Relative Permittivity		
P-Band		
Organic Layer	8.46 -j0.99	3.29 -j0.36
Mineral Soil	8.56 -j0.75	8.96 -j0.73
L-Band		
Organic Layer	5.52 -j0.51	2.49 -j0.13
Mineral Soil	8.36 -j0.68	12.53 -j1.13
C-Band		
Organic Layer	4.09 -j0.72	2.78 -j0.42
Mineral Soil	8.45 -j1.83	11.34 -j3.50

3.0 Radiative Transfer Modeling of Forest Stands Using MIMICS

The Michigan Microwave Canopy Scattering Model (MIMICS) is a fully polarimetric, first-order radiative transfer model developed for modeling radar backscatter from tree canopies. The version of MIMICS applied in this study has been developed for forests with continuous, or nearly continuous crown layers [2]. The model requires a number of sensor and scene parameters. The sensor parameters include frequency, polarization and angle of incidence. The scene parameters consist of two types: geometric and dielectric. The geometric parameters specify the gross canopy architecture (such as the number and size distributions of various types of trees), the tree architecture (such as the sizes, shapes and orientation angles of trunks, branches and leaves) and the roughness at the air/soil boundary. The dielectric parameters include the relative permittivity of each constituent medium (soil, snow, trunks, branches and foliage) at a given frequency of interest.

The MIMICS model divides the composite scene into three general, horizontal layers as shown in Figure 7: (1) a crown layer consisting of branches and foliage, (2) a trunk layer and (3) a ground layer that also includes snow cover when present. The scattered intensity is related to the incident intensity by a canopy transformation matrix. The first-order solution of the transformation matrix consists of a summation of the scattering mechanisms shown in Figure 8. Mechanisms 1 and 2 represent interactions of the propagating intensity between the crown layer and the ground. Mechanism 3 represents an interaction between the trunk layer and the ground. Mechanisms 4 and 5 represent direct backscatter from the crown layer and the soil layer, respectively. Each of these terms depends upon the phase and extinction matrices of the canopy layers. The model produces estimates of the transmissivity through each of the canopy layers and also the backscatter arising from the various scattering pathways depicted in Figure 8.

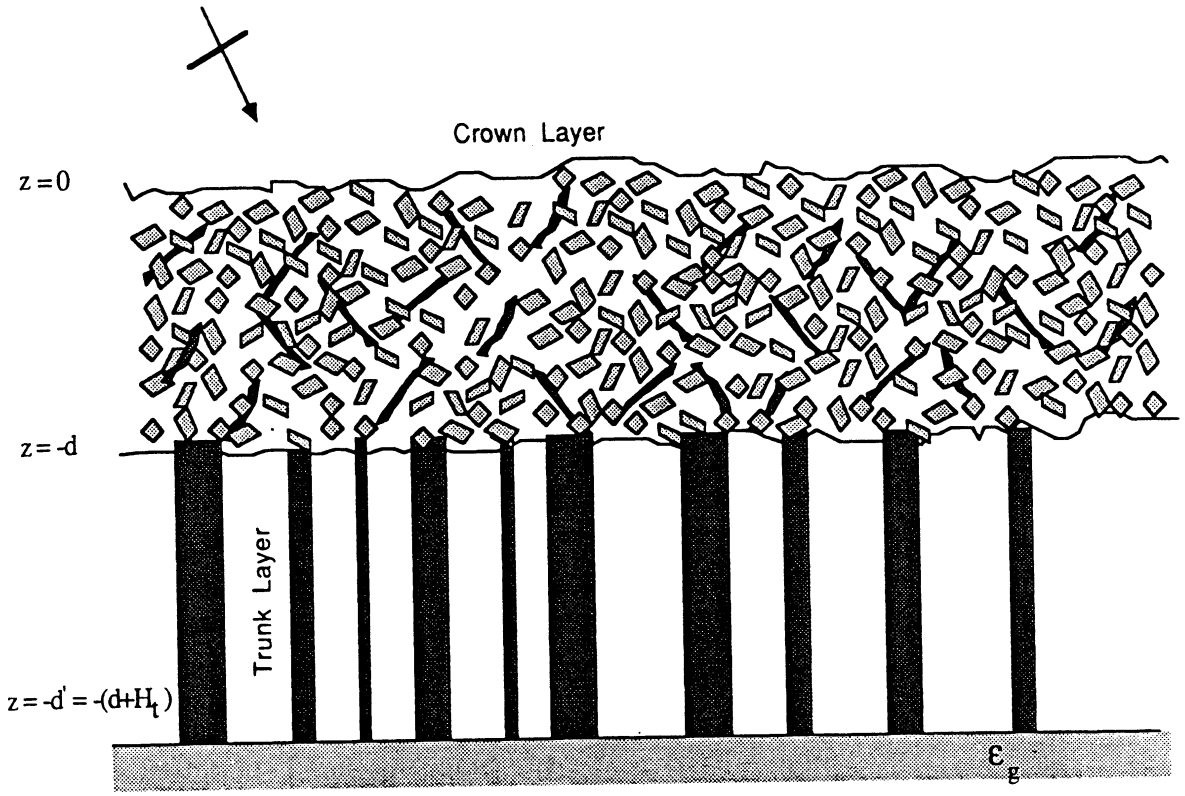

Figure 7. Forest-canopy model.

3.1 Model Description

The model is fully described in [2]. A brief overview is provided here along with variations to the model as given in [2].As a first-order model, MIMICS includes those scattering processes that involve single scattering by each layer and double scattering by pairs of layers. Since the trunks are treated as near-vertical cylinders with smooth surfaces and uniform cross-section, they will not backscatter directly except for horizontal propagation. Also, backscattering contributions involving both the trunk and crown regions are not included as this requires processes involving triple scattering.

The basic geometry of the model is depicted in Figure 9. The crown layer of leaves and branches is assumed to be continuous in the horizontal direction and statistically homogeneous over the crown volume. The upper and lower boundaries of the crown layer are assumed to be diffuse. The trunk layer is assumed to consist of near-vertical, homogeneous dielectric cylinders with smooth outer surfaces. The air/soil boundary is treated as a specular surface.

Within the vegetation layers, the constituent elements (trunks, branches and leaves) are partitioned into classes based upon size and shape distributions. These classes are modeled as collections of dielectric cylinders or disks. The phase and extinction matrices that describe the scattering and extinction properties of each layer incorporate the distribution functions describing the size and orientation parameters of the various constituent classes. For a vegetation layer of K classes, the phase matrix of the layer is specified by:

$$\mathbf{P}(\theta_s,\phi_s;\theta_i,\phi_i)=\sum_{k=1}^{K}N_k\iint f_k(\mathbf{A};\Omega)\mathbf{L}_k(\theta_s,\phi_s;\theta_i,\phi_i;\mathbf{A};\Omega)d\mathbf{A}d\Omega \qquad (3)$$

where the summation over k represents an addition over the K constituent classes within the layer, N_k is the number of elements per unit volume of each constituent class, and $\mathbf{L}_k$ is the Stokes matrix for constituent k. The phase matrix describes the scattering by a volume of vegetation for radiation incident form the direction (θ_i, ϕ_i) and scattered into the direction (θ_S, ϕ_S). The probability density function (PDF) f_k (A; Ω) specifies the distribution over the size parameters specified by A and the orientation parameters specified by Ω for constituents in class k..

Similarly, the elements of the extinction matrix for the layer are dependent on the summation:

$$M_{mn}=\sum_{k=1}^{K}\frac{i2\pi N_k}{k_o}\left\langle \mathbf{S}_{mnk}(\theta_s,\phi_s;\theta_i,\phi_i;\mathbf{A};\Omega)\right\rangle \qquad (4)$$

where $m,n = v,h$, k_0 is the free space wave number, $(\theta_S, \phi_S) = (\theta_i, \phi_i)$, S_{mnk} is the component of the scattering matrix corresponding to polarization mn for constituent k, and the symbol < ··· > represents statistical averaging over the size and orientation distribution of the constituent class.

Several electromagnetic models are implemented in MIMICS for computing the phase and extinction matrices. Three cylinder scattering models are used to model the trunks, branches and stems. The largest size classes of cylindrical elements (relative to wavelength) use a scattering model based on an exact solution for an infinitely long

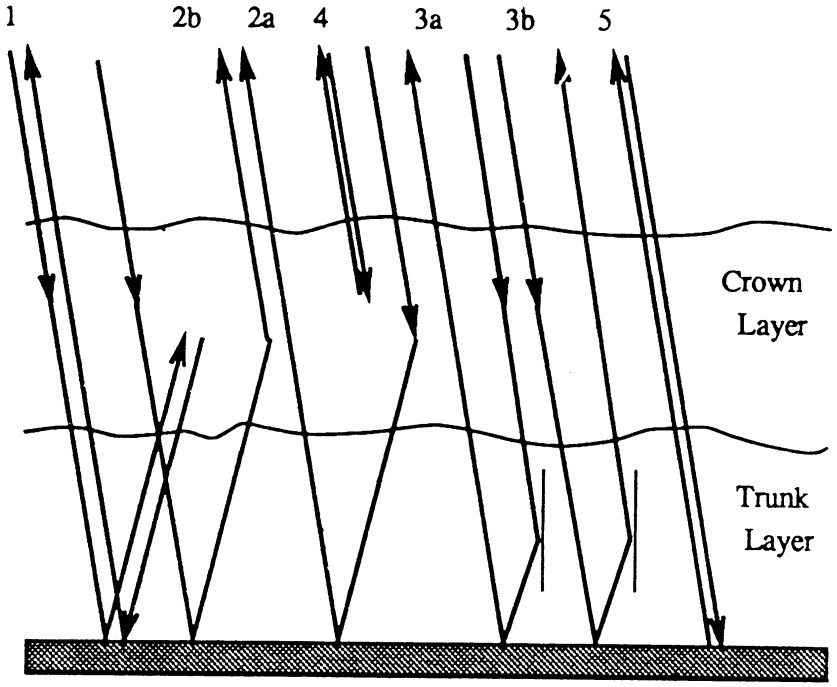

Figure 8. Scattering mechanisms considered by the first-order, radiative transfer solution.

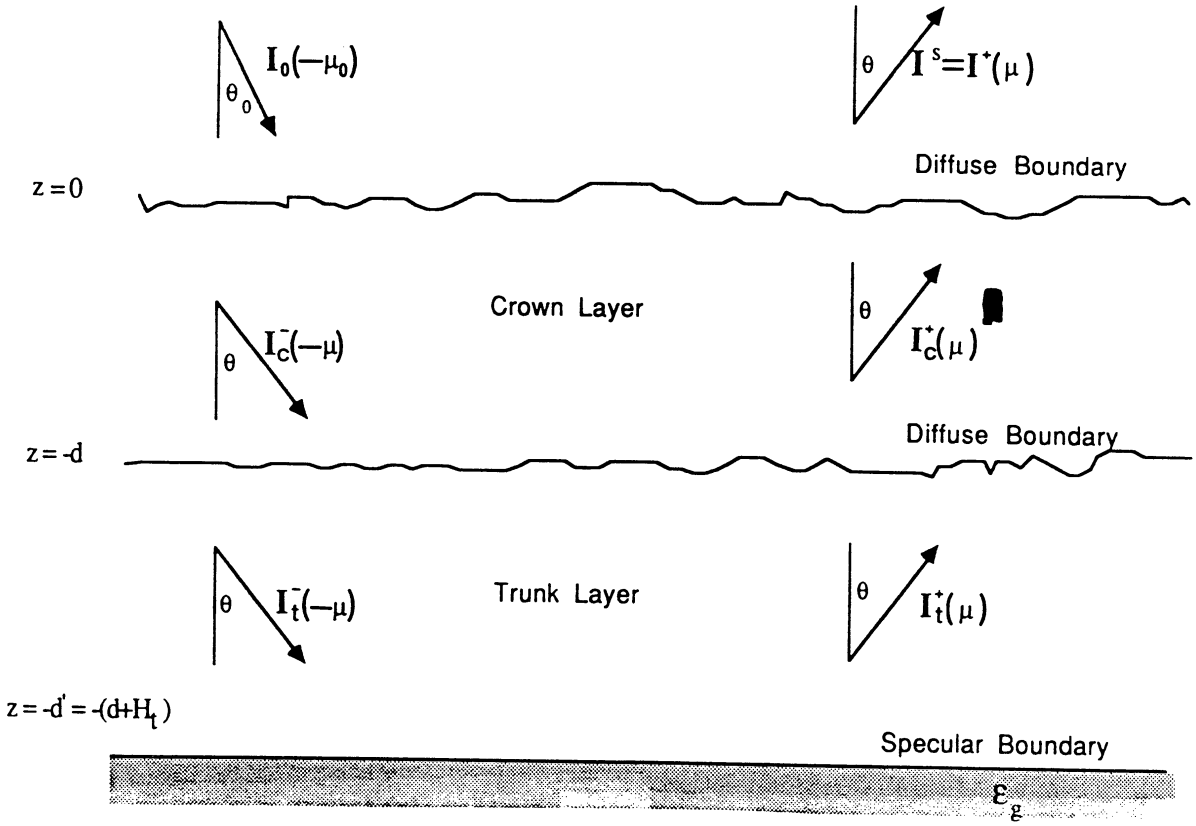

Figure 9. Geometry of the radiative transfer model.

homogeneous dielectric cylinder [14] with a stationary phase approximation to find the solution for a finite cylinder. Long, thin cylinders are modeled with a technique that extends Rayleigh scattering theory to cylindrical bodies with lengths greater than the incident wavelength [15]. Smaller cylindrical constituents are modeled using a solution for small prolate spheroids [16]. The electromagnetic properties of leaves are modeled using either a physical optics model for a dielectric disk [17] or a Rayleigh solution for small oblate spheroids [16]. The specific choice of model for a particular constituent class is based on the size parameters of that class relative to the radar frequency.

For backscatter from the soil surface, three scattering models can be employed depending upon roughness relative to wavelength: (1) the Kirchhoff model under the stationary-phase approximation (geometrical optics model), (2) the Kirchhoff model under the scalar approximation (the physical optics model) and (3) the small perturbation model. The correlation length of the soil surface is assumed to be relatively small; therefor, the small perturbation model is used at P-band for the forest stands encountered in this study.

Scattering mechanisms involving interaction of another layer with bistatic scattering from the soil (mechanisms 1 to 3 in Figure 8) assume the soil to be a specular surface. For bistatic scattering from the soil surface in the specular direction, the effects of surface roughness are to reduce scatter according to:

$$\Gamma_s = \Gamma_o \exp(-2k_o S\cos\theta)^2 \qquad (5)$$

where Γ_o is the reflection coefficient for a smooth surface in the specular direction, k_o is the free space wave number and S is the root-mean-square surface roughness. This function has a negligible effect at P-band since we assume S=1 cm for these forest stands. Γ_o is calculated on the basis of the dielectric properties of the mineral soil; the presence of the thin layer of organic material is ignored in these simulations
In addition, scattering mechanisms 2 and 3, the ground/trunk interactions and the ground/crown interactions, both involve reciprocal paths. These two paths are assumed to add coherently.

Snow is treated as a homogeneous dielectric layer over the mineral soil surface with a diffuse upper boundary. At long wavelengths, such as P- and L-bands, the snow layer behaves as an attenuator with negligible backscattering. The dielectric properties of snow vary as functions of moisture, density and temperature. Since the April 1992 SAR overflights all occurred at temperatures below zero, snow moisture = 0. Hence the dielectric properties of the snow cover in April can be estimated from measured snow temperature and density using [18]:

$$\varepsilon' = 1 + 2.2\rho_d \qquad (6)$$

$$\tan\delta_d = \varepsilon''/\varepsilon' = 1.59*10^6*\left(0.52\rho_d + 0.62\rho_d{}^2\right)$$
$$\left(f^{-1} + 1.23*10^{-14}\sqrt{f}\right)e^{0.036T}/\left(1 + 1.7\rho_d + 0.7\rho_d{}^2\right) \qquad (7)$$

where ρ_s is the density of the snow in g/cm^3, f the frequency in Hz, and T the snow temperature in °C. For an average snow density of 0.351 g/cm^3 and T=0 in April 1992, Eq. (6-7) yield ε*= (1.77, 1.075 E-3) at 450 MHz.

3.2 Simulated Transmissivity and Backscatter

The forest stand characteristics during the April and July 1992 experimental periods are used to parameterized the MIMICS model. A summary of the MIMICS input parameters is given in Table 13 for Stands G, O, Q and T. The biometric survey data determines the density of trees per specie within a stand and also the height and diameter distributions of the trunk layer. Allometric equations are used on a per tree basis within each stand to estimate dry biomass quantities as functions of height and diameter and then integrated over the stand. The biomass values are used in conjunction with the size and specific densities of the constituent classes (leaves and two branch classes - primary and secondary) to estimate the number of scattering elements of the constituent class per unit volume within the crown layer. Dielectric properties are either measured directly or are estimated from measured moisture, density and temperature of a given constituent class of vegetation, soil or snow. The soil surface roughness is assumed to be relatively smooth and the same for all stands. The orientation functions for the vegetation constituent classes are assumed to have uniform distributions unless field measurements are available which indicate otherwise.

The MIMICS model yields estimates of one-way transmissivity τ and net backscatter. Transmissivity is calculated for each of the two canopy layers (crown and trunk layer) and summed to yield net transmissivity. Backscatter is calculated for each of the first-order mechanisms illustrated in Figure 8 and summed to yield net backscatter. The input parameters specified in Table 13 were used in MIMICS with sensor parameters of P-band (440 MHz), from 20° to 60° angle of incidence and for all linear polarizations. Tables 14 to 17 give the model results for the four forest stands (G, O, Q and T), respectively. Each table has two parts, one each for the April and July observation periods.

The MIMICS estimates of τ are plotted versus angle of incidence θ in Figures 10 to 13 for Stands G, O, Q and T, respectively. In general, τ decreases with angle θ since path length through a layer increases as $d\cos\theta$, where d is the layer thickness. For the crown layer, $\tau_h \approx \tau_v$. For the trunk layer, $\tau_h > \tau_v$ and the difference increases with θ. The coupling of the propagating wave with the array of near-vertical trunks is strongest for V polarization. As a consequence, the total one-way transmissivity of the canopy is shown to be greater for H polarized waves. For H polarized waves, $\tau_{trunk} > \tau_{crown}$. Extinction within the crown layer is mainly caused by the large primary branch class. For V polarized waves, τ_{trunk} is usually less than τ_{crown} during the April period; but $\tau_{trunk} > \tau_{crown}$ during the July period due to increases in foliage and higher dielectric constants of the branches during the summer. Transmissivity is not found to vary versus season in a consistent fashion for all stands. For Stands G and Q, $\tau_{April} < \tau_{July}$, while the reverse is found to be predicted by MIMICS for Stands O and T. It is important to note that none of the simulations are for frozen conditions of winter.

The net backscatter $\sigma°$ estimates listed in Tables 14 to 17 are plotted in Figures 14 to 17 for Stands G, O, Q and T, respectively. For Stand G, $\sigma°$ is shown in Figure 14 to be very similar for the two observation periods, especially for $\theta<40°$. As indicated in Table 13, there are only minor differences in the dielectric properties of the vegetation constituents between the two periods; the dielectric loss is greater in July. The major difference is in the surface layer properties. In April, a 35.9 cm dry snow layer overlies

Table 13 Summary of MIMICS input parameters.

	Stand G	Stand O	Stand Q	Stand T
Forest type	Red pine	Northern hardwood	Maple	Maple/Aspen
Dry Biomass (kg/m^2)				
Total				
Apr-92	18.233	20.266	14.713	21.119
Jul-92	18.282	20.546	15.009	21.675
Trunk	15.211	15.728	12.375	17.390
Branch	2.239	4.496	2.338	3.729
Foliar	0.832	0.323	0.288	0.556
Stems per hectare	1018	925	1842	1762
No. of tree classes	8	9	5	9
Mean trunk height of upper stratum (m)	15.7	16.1	13.7	11.4
Mean trunk diameter of upper stratum (cm)	17.9	17.5	11.1	11.0
Mean crown thickness (m)	8.5	7.4	8.7	6.5
Crown layer geometry				
Leaves				
Thickness (cm)	0.074	0.100	0.100	0.100
Length (cm)	12.50	6.40	6.99	5.79
Mass (g)	0.026	0.370	0.374	0.367
Density (no./m^3)				
Apr-92	3838.52	0.00	0.00	0.00
Jul-92	3838.52	118.08	88.44	233.12
Primary branches				
Length (m)	0.73	2	2	2
Diameter (cm)	0.99	1.5	1.5	1.5
Mass (g)	23.43	189.44	166.82	151.97
Density (no./m^3)	7.49	2.14	1.07	2.52
Secondary branches				
Length (m)	0.33	1	1	1
Diameter (cm)	0.57	0.75	0.75	0.75
Mass (g)	3.51	23.68	20.85	19
Density (no./m^3)	25	8.55	4.3	8.55
Canopy moistures or (dielectric @ P-band)				
Trunk				
Apr-92	(36.48,-j6.23)	(27.41,-j3.93)	(27.41,-j3.93)	(20.98,-j3.24)
Jul-92	(36.26,-j8.45)	(28.26,-j7.52)	(35.51,-j9.36)	(28.26,-j7.52)
Leaves	(17.1,-j3.2)	0.5734	0.5796	0.5835
Branches				
Apr-92	(36.48,-j6.23)	(27.41,-j3.93)	(27.41,-j3.93)	(20.98,-j3.24)
Jul-92	(36.26,-j8.45)	(28.26,-j7.52)	(35.51,-j9.36)	(28.26,-j7.52)
Temperature (°C)				
Apr-92	1.4	1.0	1.0	1.0
Jul-92	12.4	7.5	7.5	7.5
Wood density (g/cm^3)	0.417	0.536	0.472	0.43
Soil moisture or (dielectric @ P-band)				
Apr-92	0.472	0.467	0.467	0.467
Jul-92	0.137	0.139	0.139	0.139
Soil temperature (°C)				
Apr-92	1.4	1	1	1
Jul-92	12.4	7.5	7.5	7.5
Soil Texture				
% Sand	90	50	60	60
% Clay	0	10	10	10
RMS roughness (cm)	1	1	1	1
Correlation length (cm)	15	15	15	15
Snow depth in April (cm)	35.9	25.4	25.4	25.4
Snow dielectric @ P-band	(1.77,-j.0011)	(1.77,-j.0011)	(1.77,-j.0011)	(1.77,-j.0011)
Orientation functions				
Secondary branches	0.5sin(theta)	1.23sin(theta-30)**9	1.23sin(theta-30)**9	1.23sin(theta-30)**9
Primary branches		uniform = 0.5sin(theta)		
Leaves		uniform = 0.5sin(theta)		
Trunk		1.164cos (theta**8)		

Table 14. One-way transmissivity and radar backscatter coefficient for Stand G

(a) Stand G - April 1992 - P band

Incidence Angle (degrees)			20	25	30	35	40	45	50	55	60
1-Way Tau	Total:	H	0.562	0.549	0.532	0.510	0.484	0.452	0.414	0.368	0.314
		V	0.517	0.490	0.461	0.428	0.391	0.351	0.307	0.258	0.205
	Crown:	H	0.657	0.646	0.633	0.617	0.597	0.572	0.541	0.502	0.453
		V	0.656	0.646	0.633	0.616	0.596	0.570	0.539	0.500	0.451
	Trunk:	H	0.856	0.849	0.839	0.827	0.811	0.790	0.765	0.734	0.694
		V	0.789	0.759	0.728	0.694	0.657	0.616	0.570	0.517	0.455
Sigma0 (dB)	HH:	Total	**-4.57**	**-4.35**	**-3.80**	**-3.18**	**-2.78**	**-2.70**	**-3.02**	**-3.68**	**-4.81**
		Crwn-Gnd	-16.83	-17.38	-17.99	-18.66	-19.38	-20.17	-21.09	-22.21	-23.65
		Trunk-Gnd	-5.11	-4.82	-4.17	-3.46	-3.00	-2.89	-3.20	-3.86	-5.01
		Direct Crwn	-18.88	-18.94	-19.01	-19.11	-19.23	-19.38	-19.58	-19.83	-20.17
		Direct Gnd	-21.64	-22.39	-23.32	-24.43	-25.71	-27.18	-28.86	-30.80	-33.08
		Gnd-Cn-Gnd	-32.76	-32.95	-33.22	-33.62	-34.16	-34.91	-35.93	-37.33	-39.29
	VV:	Total	**-9.79**	**-7.73**	**-6.67**	**-6.18**	**-6.13**	**-6.53**	**-7.25**	**-8.42**	**-10.11**
		Crwn-Gnd	-23.52	-27.40	-30.56	-31.35	-30.87	-30.46	-30.48	-31.04	-32.28
		Trunk-Gnd	-10.97	-8.31	-7.07	-6.51	-6.44	-6.84	-7.59	-8.82	-10.64
		Direct Crwn	-18.88	-18.94	-19.01	-19.11	-19.23	-19.39	-19.57	-19.81	-20.13
		Direct Gnd	-21.45	-21.99	-22.64	-23.42	-24.36	-25.49	-26.87	-28.60	-30.84
		Gnd-Cn-Gnd	-34.68	-35.67	-36.83	-38.18	-39.79	-41.71	-44.05	-46.97	-50.73
	HV:	Total	**-14.83**	**-15.48**	**-16.71**	**-17.77**	**-18.77**	**-19.92**	**-20.81**	**-21.68**	**-22.60**
		Crwn-Gnd	-24.85	-26.32	-27.63	-28.72	-29.68	-30.66	-31.80	-33.24	-35.14
		Trunk-Gnd	-15.92	-16.57	-18.04	-19.36	-20.69	-22.36	-23.67	-24.99	-26.41
		Direct Crwn	-24.11	-24.17	-24.24	-24.34	-24.46	-24.62	-24.81	-25.07	-25.40
		Direct Gnd	-48.53	-47.65	-47.24	-47.17	-47.34	-47.72	-48.29	-49.05	-50.09
		Gnd-Cn-Gnd	-38.92	-39.49	-40.19	-41.04	-42.09	-43.40	-45.03	-47.13	-49.89

Table 14. Continued

(b) Stand G - July 1992 - P band

Incidence Angle (degrees)			20	25	30	35	40	45	50	55	60
1-Way Tau	Total:	H	0.695	0.683	0.667	0.646	0.620	0.589	0.552	0.506	0.452
		V	0.641	0.611	0.578	0.543	0.505	0.462	0.414	0.360	0.300
	Crown:	H	0.799	0.793	0.784	0.773	0.760	0.742	0.721	0.693	0.656
		V	0.799	0.792	0.784	0.773	0.759	0.741	0.719	0.691	0.654
	Trunk:	H	0.870	0.862	0.850	0.835	0.816	0.793	0.765	0.731	0.689
		V	0.803	0.771	0.738	0.703	0.665	0.623	0.575	0.521	0.459
Sigma0 (dB)	HH:	Total	**-5.68**	**-5.06**	**-3.96**	**-2.84**	**-2.00**	**-1.56**	**-1.41**	**-1.57**	**-2.09**
		Crwn-Gnd	-17.44	-17.81	-18.21	-18.62	-19.02	-19.42	-19.87	-20.42	-21.15
		Trunk-Gnd	-6.33	-5.57	-4.32	-3.09	-2.19	-1.72	-1.55	-1.71	-2.23
		Direct Crwn	-18.70	-18.74	-18.78	-18.83	-18.90	-18.99	-19.11	-19.26	-19.47
		Direct Gnd	-22.58	-23.68	-25.05	-26.68	-28.59	-30.81	-33.38	-36.40	-39.99
		Gnd-Cn-Gnd	-34.33	-34.21	-34.10	-34.03	-34.01	-34.09	-34.32	-34.78	-35.61
	VV:	Total	**-9.26**	**-7.23**	**-6.36**	**-6.08**	**-6.30**	**-7.00**	**-8.17**	**-9.85**	**-12.40**
		Crwn-Gnd	-24.54	-28.54	-31.93	-33.02	-32.80	-32.72	-33.24	-34.60	-37.19
		Trunk-Gnd	-11.11	-8.27	-7.18	-6.84	-7.05	-7.83	-9.15	-11.23	-14.49
		Direct Crwn	-14.40	-14.21	-14.13	-14.17	-14.37	-14.72	-15.20	-15.58	-16.61
		Direct Gnd	-29.26	-30.22	-31.39	-32.82	-34.57	-36.72	-39.38	-42.76	-47.17
		Gnd-Cn-Gnd	-40.65	-42.05	-43.88	-46.26	-49.31	-53.23	-58.28	-64.93	-73.79
	HV:	Total	**-15.29**	**-15.78**	**-16.79**	**-17.69**	**-18.54**	**-19.49**	**-20.20**	**-20.89**	**-21.57**
		Crwn-Gnd	-26.02	-27.60	-29.04	-30.30	-31.49	-32.80	-34.40	-36.49	-39.27
		Trunk-Gnd	-16.37	-16.84	-18.03	-19.14	-20.23	-21.55	-22.55	-23.53	-24.54
		Direct Crwn	-24.03	-24.07	-24.11	-24.17	-24.24	-24.33	-24.44	-24.59	-24.79
		Direct Gnd	-49.74	-48.99	-48.80	-49.01	-49.55	-50.35	-51.42	-52.78	-54.52
		Gnd-Cn-Gnd	-41.04	-41.59	-42.25	-43.08	-44.14	-45.52	-47.33	-49.76	-53.07

Table 15. One-way transmissivity and radar backscatter coefficient for Stand O

(a) Stand O - April 1992 - P band

Incidence Angle (degrees)			20	25	30	35	40	45	50	55	60
1-Way Tau	Total:	H	0.508	0.494	0.476	0.453	0.426	0.393	0.354	0.309	0.264
		V	0.474	0.450	0.422	0.392	0.357	0.319	0.277	0.231	0.182
	Crown:	H	0.597	0.586	0.571	0.553	0.531	0.504	0.470	0.429	0.390
		V	0.598	0.588	0.574	0.557	0.536	0.510	0.478	0.439	0.390
	Trunk:	H	0.850	0.843	0.833	0.819	0.802	0.781	0.754	0.720	0.677
		V	0.793	0.766	0.736	0.703	0.667	0.626	0.580	0.527	0.466
Sigma0 (dB)	HH:	Total	**-4.78**	**-4.93**	**-4.83**	**-4.57**	**-4.41**	**-4.48**	**-4.81**	**-5.49**	**-6.64**
		Crwn-Gnd	-13.01	-13.97	-14.85	-15.72	-16.60	-17.57	-18.68	-20.03	-21.76
		Trunk-Gnd	-6.04	-6.04	-5.76	-5.33	-5.04	-5.04	-5.33	-6.01	-7.21
		Direct Crwn	-15.69	-15.75	-15.82	-15.92	-16.06	-16.23	-16.45	-16.74	-17.12
		Direct Gnd	-22.54	-23.34	-24.32	-25.48	-26.84	-28.41	-30.23	-32.35	-34.88
		Gnd-Cn-Gnd	-30.56	-30.79	-31.12	-31.59	-32.23	-33.11	-34.32	-35.97	-38.27
	VV:	Total	**-12.17**	**-10.20**	**-8.97**	**-8.33**	**-8.18**	**-8.45**	**-9.09**	**-10.13**	**-11.60**
		Crwn-Gnd	-27.04	-29.62	-29.64	-29.13	-28.23	-27.77	-27.80	-28.44	-29.82
		Trunk-Gnd	-15.53	-11.92	-10.16	-9.30	-9.08	-9.37	-10.10	-11.32	-13.18
		Direct Crwn	-15.59	-15.61	-15.66	-15.75	-15.88	-16.07	-16.32	-16.65	-17.00
		Direct Gnd	-25.92	-26.67	-27.61	-28.77	-30.19	-31.94	-34.12	-36.87	-40.44
		Gnd-Cn-Gnd	-32.16	-33.08	-34.19	-35.54	-37.17	-39.16	-41.60	-44.67	-48.55
	HV:	Total	**-15.61**	**-16.05**	**-16.76**	**-17.42**	**-18.14**	**-18.92**	**-19.66**	**-20.41**	**-21.21**
		Crwn-Gnd	-24.82	-25.91	-26.54	-27.11	-27.74	-28.54	-29.60	-31.04	-33.00
		Trunk-Gnd	-17.97	-18.50	-19.64	-20.81	-22.18	-23.84	-25.51	-27.31	-29.28
		Direct Crwn	-20.96	-20.99	-21.05	-21.13	-21.25	-21.42	-21.64	-21.93	-22.32
		Direct Gnd	-50.29	-49.38	-48.94	-48.84	-49.01	-49.40	-50.01	-50.86	-52.03
		Gnd-Cn-Gnd	-36.64	-37.20	-37.90	-38.78	-39.89	-41.28	-43.05	-45.33	-48.35

Table 15. Continued

(b) Stand O - July 1992 - P band

Incidence Angle (degrees)			20	25	30	35	40	45	50	55	60
1-Way Tau	Total:	H	0.431	0.417	0.399	0.376	0.349	0.317	0.280	0.238	0.190
		V	0.402	0.379	0.353	0.324	0.292	0.257	0.218	0.177	0.134
	Crown:	H	0.508	0.495	0.480	0.460	0.436	0.406	0.371	0.330	0.280
		V	0.509	0.497	0.482	0.463	0.440	0.412	0.378	0.337	0.288
	Trunk:	H	0.849	0.842	0.832	0.819	0.802	0.781	0.755	0.721	0.679
		V	0.790	0.763	0.733	0.700	0.664	0.624	0.578	0.525	0.464
Sigma0 (dB)	HH:	Total	**-7.52**	**-7.64**	**-7.50**	**-7.21**	**-6.99**	**-6.99**	**-7.24**	**-7.86**	**-8.98**
		Crwn-Gnd	-15.82	-16.71	-17.48	-18.24	-19.02	-19.88	-20.90	-22.18	-23.91
		Trunk-Gnd	-9.14	-9.10	-8.76	-8.25	-7.88	-7.78	-7.99	-8.61	-9.81
		Direct Crwn	-15.78	-15.85	-15.95	-16.07	-16.24	-16.44	-16.71	-17.06	-17.50
		Direct Gnd	-26.69	-27.93	-29.47	-31.33	-33.54	-36.15	-39.24	-42.95	-47.51
		Gnd-Cn-Gnd	-35.69	-35.74	-35.84	-36.05	-36.41	-36.99	-37.87	-39.21	-41.26
	VV:	Total	**-13.52**	**-12.35**	**-11.69**	**-11.51**	**-11.78**	**-12.49**	**-13.54**	**-14.92**	**-16.37**
		Crwn-Gnd	-29.92	-32.54	-33.03	-33.05	-32.75	-33.00	-33.99	-35.99	-39.46
		Trunk-Gnd	-18.61	-15.44	-14.07	-13.66	-13.97	-14.98	-16.67	-19.31	-23.36
		Direct Crwn	-15.68	-15.72	-15.79	-15.90	-16.07	-16.30	-16.59	-16.98	-17.39
		Direct Gnd	-25.92	-26.67	-27.61	-28.77	-30.19	-31.94	-34.12	-36.87	-40.44
		Gnd-Cn-Gnd	-38.22	-39.51	-41.12	-43.14	-45.67	-48.90	-53.09	-48.71	-66.54
	HV:	Total	**-17.59**	**-17.94**	**-18.50**	**-19.04**	**-19.63**	**-20.27**	**-20.91**	**-21.57**	**-22.28**
		Crwn-Gnd	-28.05	-29.32	-30.21	-31.13	-32.23	-33.66	-35.58	-38.19	-41.78
		Trunk-Gnd	-20.98	-21.47	-22.55	-23.67	-25.01	-26.68	-28.43	-30.40	-32.68
		Direct Crwn	-21.08	-21.13	-21.21	-21.32	-21.47	-21.67	-21.94	-22.29	-22.75
		Direct Gnd	-54.05	-53.46	-53.43	-53.83	-54.60	-55.73	-57.23	-59.19	-61.79
		Gnd-Cn-Gnd	-42.28	-42.93	-44.84	-46.24	-48.08	-50.51	-53.79	-53.79	-58.27

Table 16. One-way transmissivity and radar backscatter coefficient for Stand Q

(a) Stand Q - April 1992 - P band

Incidence Angle (degrees)			20	25	30	35	40	45	50	55	60
1-Way Tau	Total:	H	0.590	0.579	0.564	0.545	0.522	0.493	0.458	0.415	0.362
		V	0.531	0.500	0.466	0.429	0.390	0.347	0.300	0.250	0.196
	Crown:	H	0.738	0.730	0.719	0.706	0.689	0.668	0.641	0.608	0.565
		V	0.739	0.731	0.721	0.709	0.693	0.673	0.648	0.616	0.574
	Trunk:	H	0.800	0.793	0.784	0.772	0.757	0.738	0.714	0.682	0.642
		V	0.719	0.683	0.646	0.606	0.563	0.516	0.464	0.406	0.342
Sigma0 (dB)	HH:	Total	**-4.04**	**-4.94**	**-5.39**	**-5.35**	**-5.03**	**-4.67**	**-4.42**	**-4.44**	**-4.86**
		Crwn-Gnd	-14.00	-14.90	-15.67	-16.42	-17.14	-17.90	-18.75	-19.76	-21.04
		Trunk-Gnd	-4.85	-5.81	-6.24	-6.09	-5.64	-5.16	-4.83	-4.80	-5.19
		Direct Crwn	-17.20	-17.23	-17.28	-17.34	-17.42	-17.52	-17.67	-17.86	-18.12
		Direct Gnd	-21.23	-21.96	-22.84	-23.88	-25.08	-26.45	-28.00	-29.78	-31.85
		Gnd-Cn-Gnd	-31.28	-31.42	-31.62	-31.91	-32.34	-32.94	-33.79	-35.00	-36.73
	VV:	Total	**-11.46**	**-9.65**	**-8.51**	**-8.00**	**-7.97**	**-8.36**	**-9.09**	**-10.23**	**-11.79**
		Crwn-Gnd	-28.35	-30.98	-31.05	-30.59	-29.74	-29.31	-29.37	-30.02	-31.39
		Trunk-Gnd	-13.71	-10.90	-9.40	-8.74	-8.67	-9.08	-9.89	-11.19	-13.10
		Direct Crwn	-17.10	-17.10	-17.12	-17.17	-17.25	-17.39	-17.56	-17.80	-18.03
		Direct Gnd	-21.25	-21.86	-22.58	-23.43	-24.43	-25.64	-27.10	-28.93	-31.28
		Gnd-Cn-Gnd	-33.55	-34.64	-35.93	-37.45	-39.26	-41.43	-44.06	-47.35	-51.48
	HV:	Total	**-14.33**	**-14.65**	**-15.21**	**-15.78**	**-16.42**	**-17.19**	**-17.96**	**-18.79**	**-19.71**
		Crwn-Gnd	-26.01	-27.11	-27.76	-28.33	-28.97	-29.75	-30.75	-32.06	-33.81
		Trunk-Gnd	-15.45	-15.77	-16.45	-17.16	-17.98	-19.00	-20.03	-21.19	-22.53
		Direct Crwn	-22.47	-22.48	-22.50	-22.54	-22.62	-22.72	-22.87	-23.07	-23.33
		Direct Gnd	-45.47	-44.60	-44.17	-44.06	-44.18	-44.50	-45.01	-45.71	-46.69
		Gnd-Cn-Gnd	-37.66	-38.25	-38.95	-39.80	-40.85	-42.15	-43.77	-45.83	-48.50

Table 16. Continued

(b) Stand Q - July 1992 - P band

Incidence Angle (degrees)			20	25	30	35	40	45	50	55	60
1-Way Tau	Total:	H	0.553	0.540	0.524	0.504	0.479	0.448	0.412	0.367	0.315
		V	0.499	0.467	0.433	0.396	0.357	0.314	0.269	0.220	0.169
	Crown:	H	0.658	0.648	0.635	0.619	0.599	0.574	0.543	0.504	0.456
		V	0.659	0.649	0.636	0.621	0.601	0.577	0.546	0.509	0.461
	Trunk:	H	0.840	0.833	0.825	0.814	0.800	0.782	0.759	0.729	0.691
		V	0.757	0.720	0.681	0.639	0.594	0.545	0.492	0.433	0.367
Sigma0 (dB)	HH:	Total	**-6.52**	**-7.08**	**-7.19**	**-6.91**	**-6.45**	**-6.03**	**-5.73**	**-5.69**	**-6.03**
		Crwn-Gnd	-14.10	-14.88	-15.53	-16.11	-16.67	-17.26	-17.92	-18.75	-19.86
		Trunk-Gnd	-8.26	-8.86	-8.84	-8.29	-7.57	-6.94	-6.49	-6.36	-6.66
		Direct Crwn	-15.16	-15.21	-15.27	-15.36	-15.47	-15.61	-15.80	-16.05	-16.38
		Direct Gnd	-24.53	-25.68	-27.10	-28.80	-30.80	-33.14	-35.89	-39.14	-43.07
		Gnd-Cn-Gnd	-33.01	-32.93	-32.87	-32.86	-32.94	-33.15	-33.57	-34.32	-35.58
	VV:	Total	**-11.90**	**-10.44**	**-9.74**	**-9.60**	**-9.96**	**-10.75**	**-11.90**	**-13.40**	**-14.99**
		Crwn-Gnd	-28.61	-31.11	-31.72	-31.76	-31.49	-31.69	-32.57	-34.40	-37.54
		Trunk-Gnd	-15.53	-12.59	-11.42	-11.15	-11.58	-12.65	-14.37	-16.99	-20.98
		Direct Crwn	-15.08	-15.09	-15.14	-15.21	-15.33	-15.50	-15.71	-16.01	-16.31
		Direct Gnd	-24.06	-24.86	-25.84	-27.02	-28.45	-30.19	-32.32	-34.98	-38.40
		Gnd-Cn-Gnd	-36.13	-37.58	-39.34	-41.50	-44.15	-47.48	-51.73	-57.33	-64.80
	HV:	Total	**-15.49**	**-15.73**	**-16.08**	**-16.57**	**-17.07**	**-17.68**	**-18.29**	**-18.99**	**-19.76**
		Crwn-Gnd	-26.53	-27.79	-28.66	-29.52	-30.52	-31.78	-33.40	-35.47	-38.01
		Trunk-Gnd	-17.72	-17.96	-18.44	-19.17	-19.93	-20.90	-21.91	-23.11	-24.52
		Direct Crwn	-20.45	-20.48	-20.52	-20.59	-20.70	-20.84	-21.03	-21.29	-21.63
		Direct Gnd	-48.76	-48.15	-48.07	-48.39	-49.05	-50.02	-51.33	-53.03	-55.29
		Gnd-Cn-Gnd	-39.83	-40.48	-41.29	-42.30	-43.57	-45.20	-47.28	-49.93	-53.21

Table 17. One-way transmissivity and radar backscatter coefficient for Stand T

(a) Stand T - April 1992 - P band

Incidence Angle (degrees)			20	25	30	35	40	45	50	55	60
1-Way Tau	Total:	H	0.540	0.529	0.517	0.501	0.482	0.457	0.428	0.391	0.345
		V	0.485	0.459	0.431	0.400	0.367	0.330	0.289	0.243	0.193
	Crown:	H	0.692	0.683	0.671	0.655	0.636	0.613	0.584	0.547	0.500
		V	0.693	0.684	0.673	0.659	0.641	0.619	0.591	0.556	0.511
	Trunk:	H	0.780	0.776	0.771	0.765	0.757	0.747	0.733	0.715	0.689
		V	0.701	0.671	0.641	0.608	0.573	0.533	0.489	0.438	0.378
Sigma0 (dB)	HH:	Total	**-3.37**	**-4.65**	**-5.89**	**-7.06**	**-8.10**	**-8.91**	**-9.40**	**-9.69**	**-10.04**
		Crwn-Gnd	-14.89	-15.79	-16.56	-17.28	-17.97	-18.69	-19.49	-20.43	-21.63
		Trunk-Gnd	-3.94	-5.33	-6.70	-8.03	-9.23	-10.14	-10.63	-10.83	-11.08
		Direct Crwn	-17.61	-17.64	-17.70	-17.77	-17.87	-17.99	-18.16	-18.39	-18.69
		Direct Gnd	-22.01	-22.73	-23.59	-24.60	-25.77	-27.09	-28.58	-30.29	-32.28
		Gnd-Cn-Gnd	-32.69	-32.80	-32.95	-33.16	-33.49	-33.95	-34.64	-35.64	-37.11
	VV:	Total	**-11.97**	**-10.96**	**-10.08**	**-9.73**	**-9.82**	**-10.28**	**-11.05**	**-12.17**	**-13.64**
		Crwn-Gnd	-28.58	-31.66	-31.93	-31.66	-30.67	-30.11	-30.02	-30.52	-31.74
		Trunk-Gnd	-14.23	-12.52	-11.25	-10.75	-10.81	-11.32	-12.22	-13.58	-15.53
		Direct Crwn	-17.51	-17.51	-17.53	-17.60	-17.70	-17.85	-18.05	-18.32	-18.59
		Direct Gnd	-22.03	-22.59	-23.25	-24.02	-24.95	-26.07	-27.44	-29.16	-31.39
		Gnd-Cn-Gnd	-34.95	-35.94	-37.09	-38.45	-40.08	-42.40	-44.46	-47.50	-51.34
	HV:	Total	**-15.51**	**-15.98**	**-16.54**	**-17.06**	**-17.62**	**-18.25**	**-18.90**	**-19.65**	**-20.51**
		Crwn-Gnd	-27.16	-28.24	-28.85	-29.39	-29.98	-30.70	-31.66	-32.92	-34.63
		Trunk-Gnd	-16.74	-17.27	-17.98	-18.65	-19.38	-20.22	-21.10	-22.11	-23.31
		Direct Crwn	-23.10	-23.12	-23.15	-23.21	-23.30	-23.42	-23.59	-23.82	-24.13
		Direct Gnd	-47.50	-46.70	-46.32	-46.24	-46.37	-46.66	-47.10	-47.72	-48.57
		Gnd-Cn-Gnd	-39.32	-39.85	-40.47	-41.22	-42.15	-43.31	-44.77	-46.66	-49.15

Table 17. Continued

(b) Stand T - July 1992 - P band

Incidence Angle (degrees)			20	25	30	35	40	45	50	55	60
1-Way Tau	Total:	H	0.397	0.384	0.368	0.349	0.325	0.297	0.264	0.226	0.182
		V	0.364	0.341	0.315	0.287	0.256	0.222	0.186	0.148	0.109
	Crown:	H	0.474	0.461	0.445	0.425	0.400	0.371	0.336	0.294	0.246
		V	0.475	0.463	0.447	0.428	0.404	0.376	0.342	0.301	0.254
	Trunk:	H	0.838	0.833	0.827	0.821	0.812	0.800	0.786	0.766	0.739
		V	0.767	0.737	0.705	0.671	0.633	0.591	0.545	0.491	0.429
Sigma0 (dB)	HH:	Total	**-9.14**	**-10.18**	**-11.06**	**-11.72**	**-12.11**	**-12.28**	**-12.34**	**-12.51**	**-13.03**
		Crwn-Gnd	-16.39	-17.26	-18.02	-18.76	-19.49	-20.30	-21.26	-22.48	-24.13
		Trunk-Gnd	-11.49	-13.01	-14.38	-15.37	-15.78	-15.62	-15.23	-15.05	-15.42
		Direct Crwn	-15.85	-15.93	-16.03	-16.17	-16.34	-16.56	-16.85	-17.21	-17.68
		Direct Gnd	-27.40	-28.64	-30.16	-32.00	-34.17	-36.72	-39.75	-43.39	-47.86
		Gnd-Cn-Gnd	-36.60	-36.61	-36.67	-36.80	-37.04	-37.47	-38.18	-39.30	-41.07
	VV:	Total	**-14.13**	**-13.64**	**-13.37**	**-13.45**	**-13.83**	**-14.49**	**-15.32**	**-16.29**	**-17.21**
		Crwn-Gnd	-30.56	-33.22	-33.80	-33.91	-33.72	-34.07	-35.18	-37.32	-40.94
		Trunk-Gnd	-20.50	-18.35	-17.37	-17.31	-17.95	-19.25	-21.25	-24.22	-28.66
		Direct Crwn	-15.75	-15.79	-15.87	-16.00	-16.17	-16.42	-16.72	-17.13	-17.57
		Direct Gnd	-26.78	-27.59	-28.59	-29.82	-31.33	-33.19	-35.50	-38.42	-42.23
		Gnd-Cn-Gnd	-39.41	-40.80	-42.52	-44.66	-47.33	-50.72	-55.10	-60.94	-68.94
	HV:	Total	**-17.87**	**-18.16**	**-18.52**	**-18.91**	**-19.36**	**-19.94**	**-20.51**	**-21.22**	**-22.02**
		Crwn-Gnd	-28.70	-30.00	-30.93	-31.90	-33.05	-34.53	-36.47	-39.05	-42.40
		Trunk-Gnd	-21.38	-21.75	-22.37	-23.03	-23.84	-24.87	-26.06	-27.57	-29.50
		Direct Crwn	-21.16	-21.22	-21.30	-21.42	-21.58	-21.87	-22.09	-22.46	-22.93
		Direct Gnd	-52.96	-52.47	-52.50	-52.95	-53.75	-54.90	-56.42	-58.42	-61.08
		Gnd-Cn-Gnd	-43.32	-43.99	-44.85	-45.94	-47.33	-49.14	-51.51	-54.64	-58.72

Figure 10. P-band transmissivity predicted by MIMIICS for Stand G.

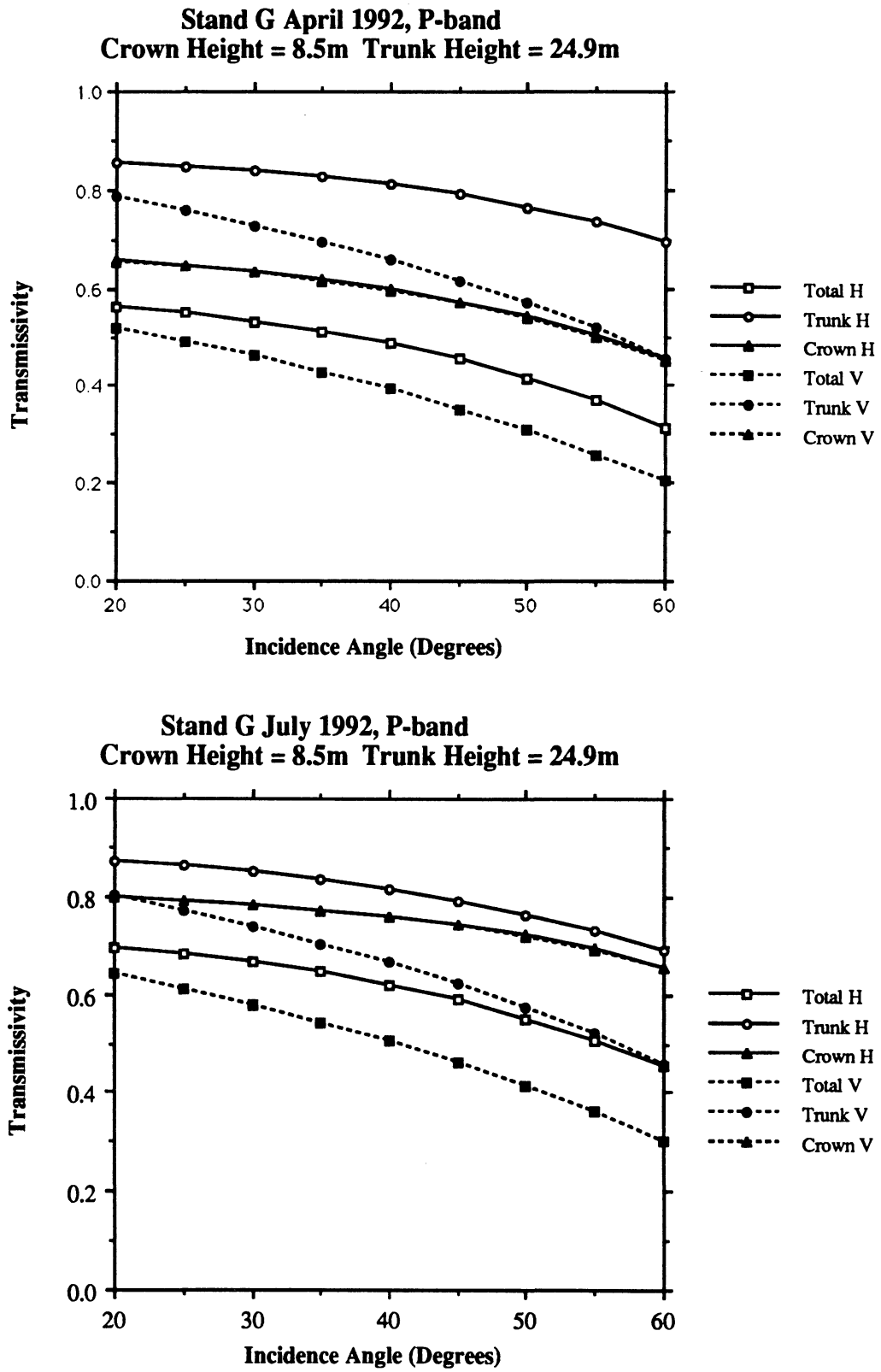

Figure 11. P-band transmissivity predicted by MIMICS for Stand O.

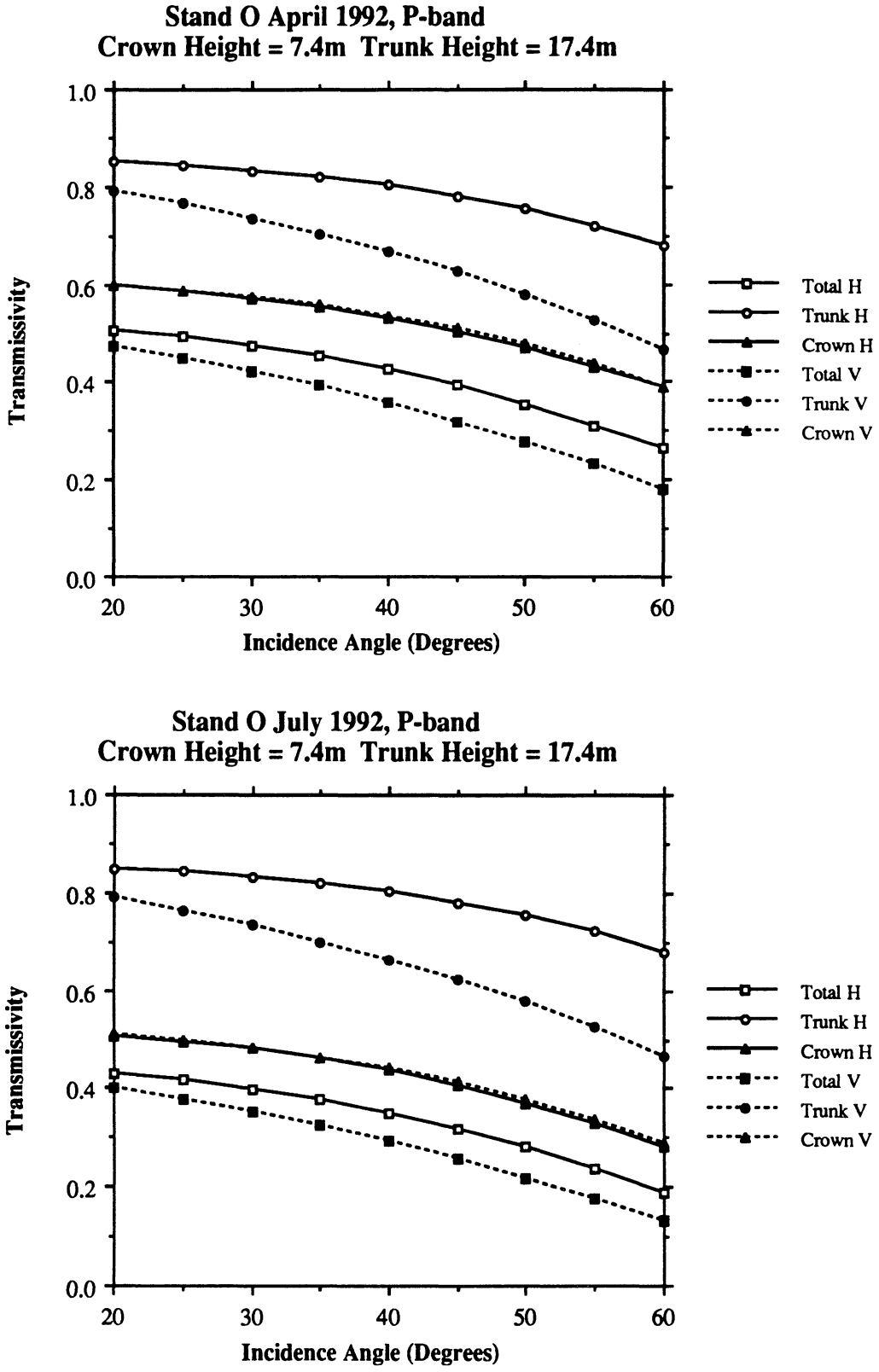

Figure 12. P-band transmissivity predicted by MIMICS for Stand Q.

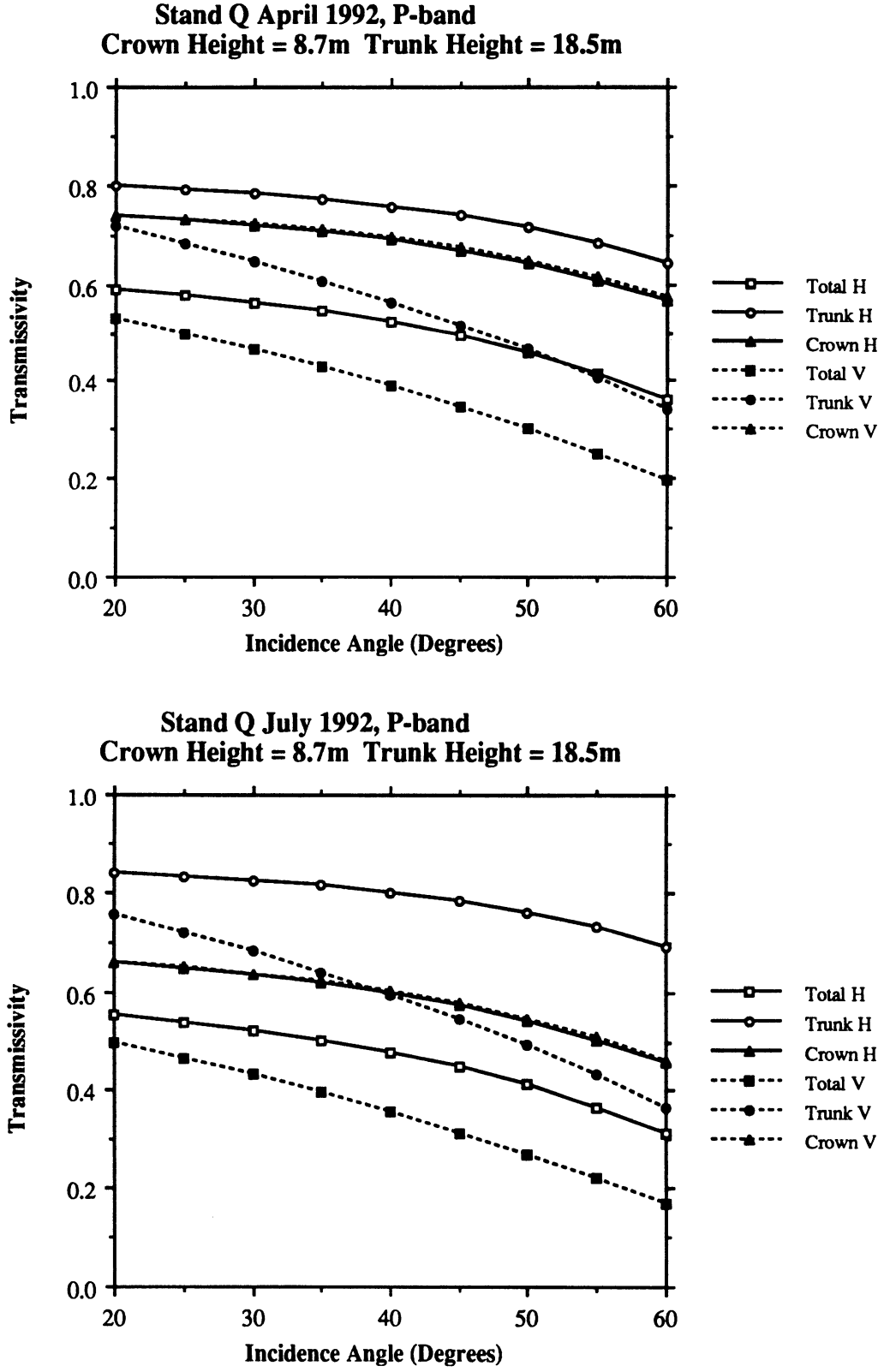

Figure 13. P-band transmissivity predicted by MIMICS for Stand T.

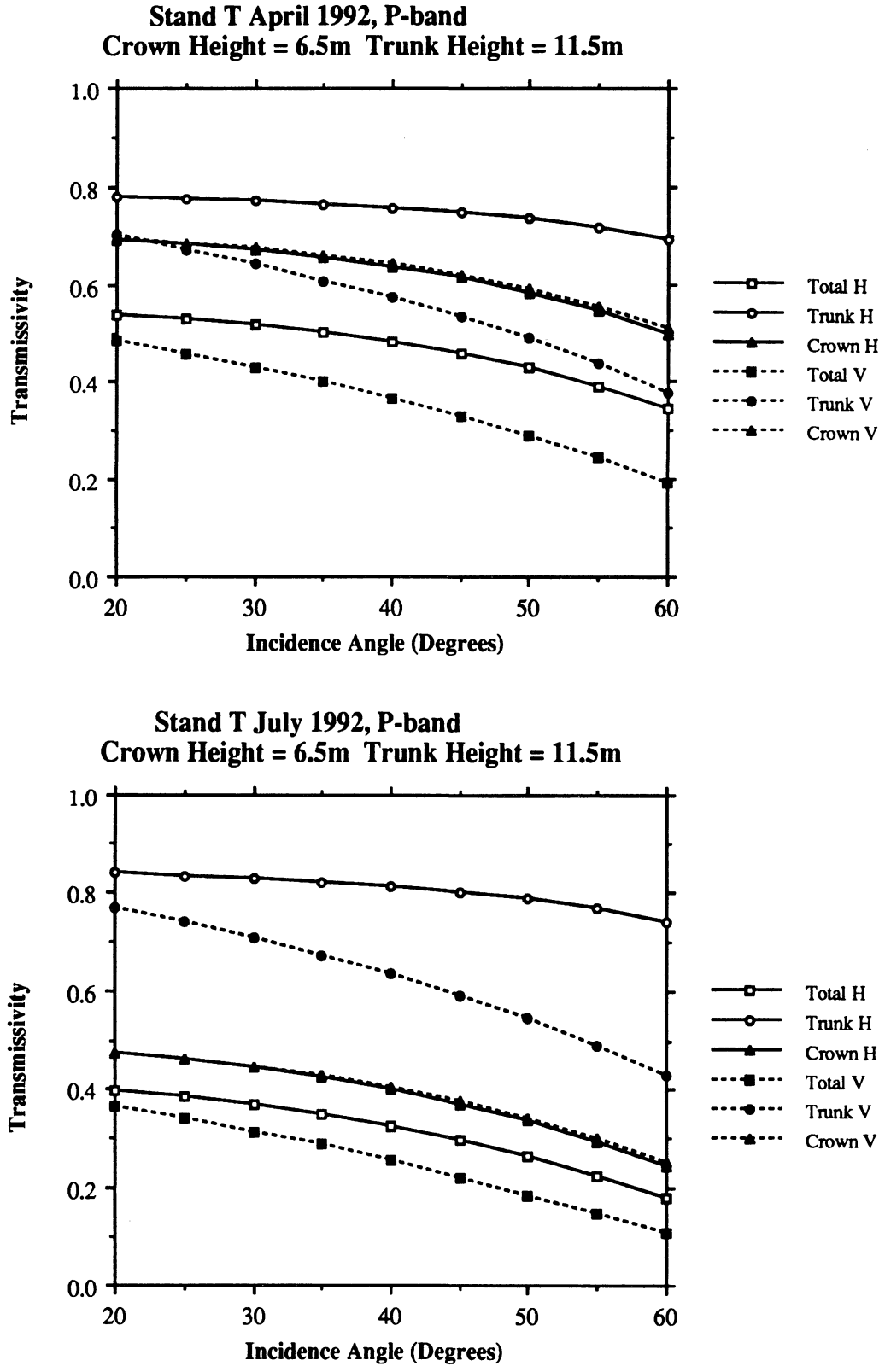

Figure 14. Net backscatter predicted by MIMICS at P-band for Stand G

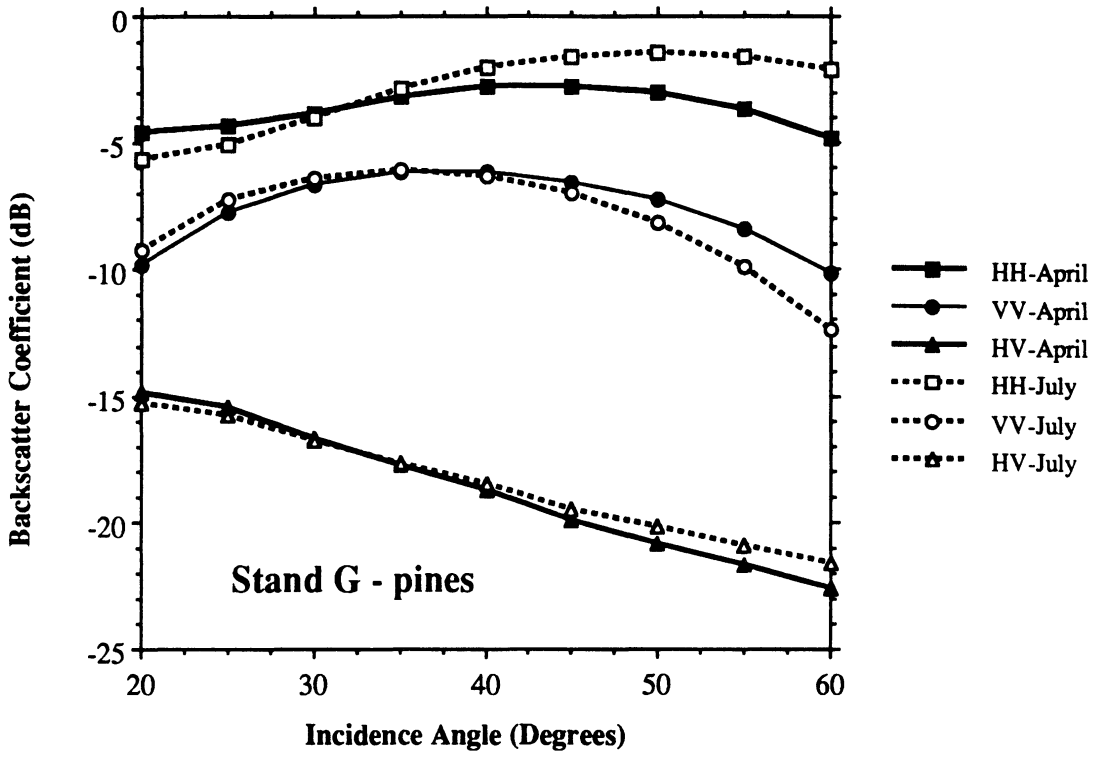

Figure 15. Net backscatter predicted by MIMICS at P-band for Stand O

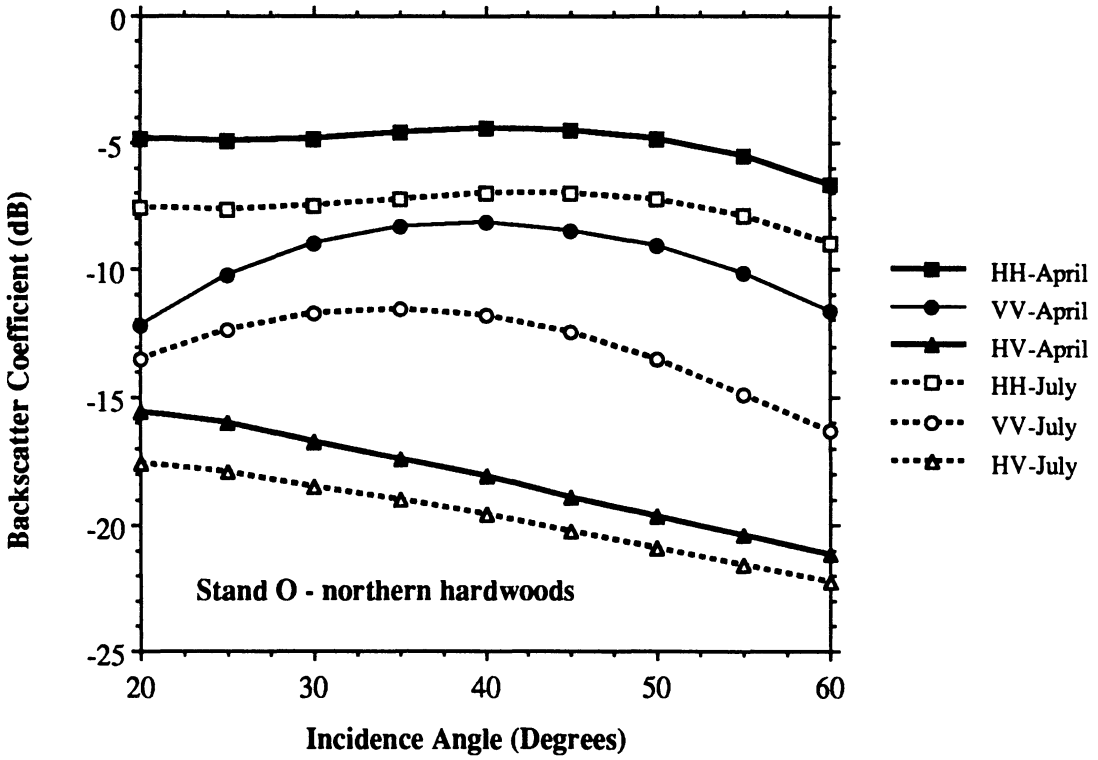

Figure 16. Net backscatter predicted by MIMICS at P-band for Stand Q

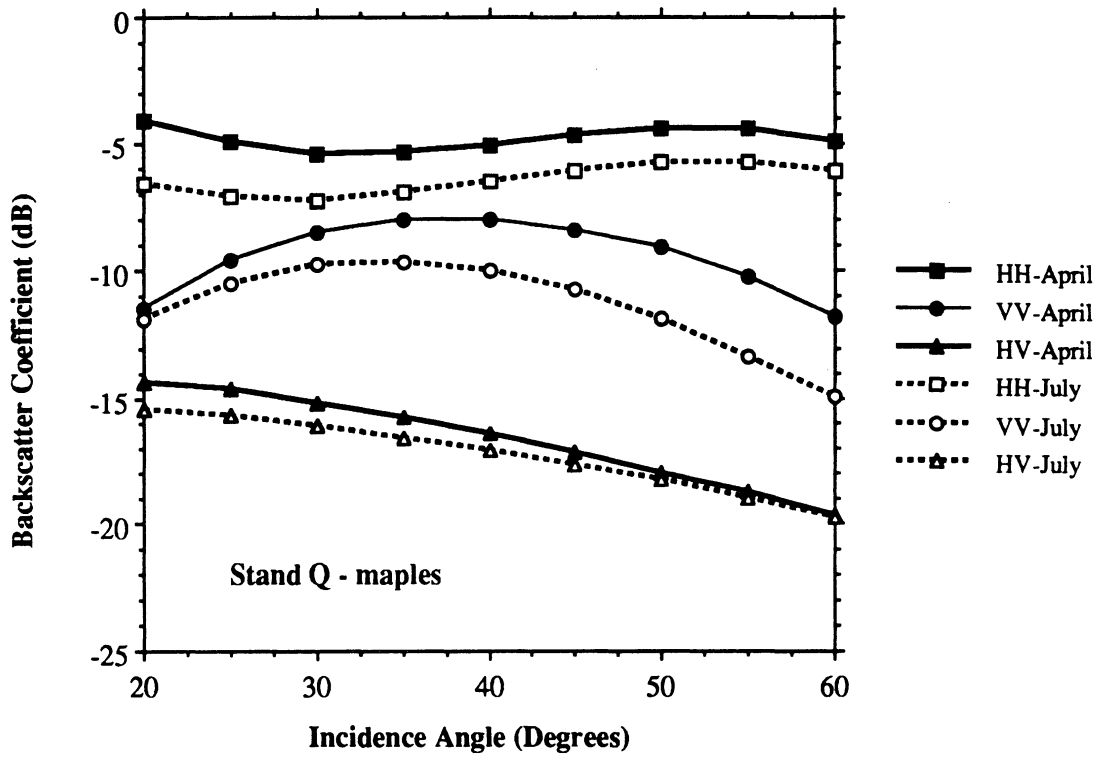

Figure 17. Net backscatter predicted by MIMICS at P-band for Stand T

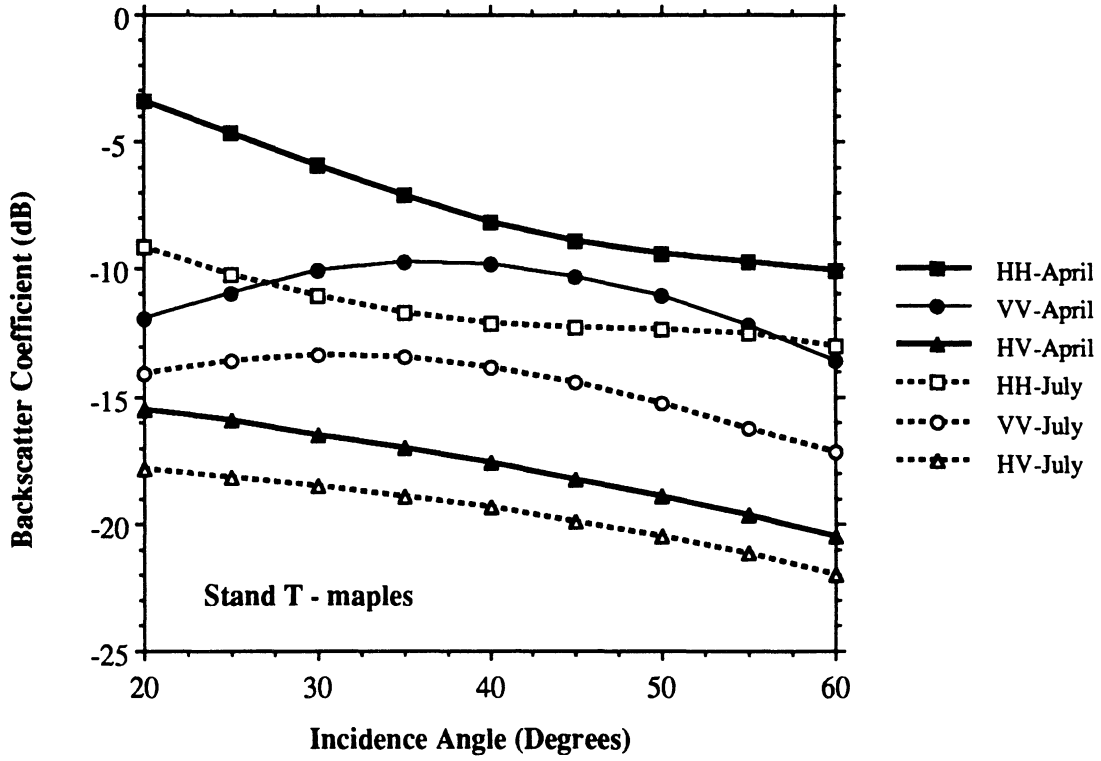

saturated soil (0.47 g/cm^3). For both observation periods, $\sigma^\circ_{hh} > \sigma^\circ_{vv}$. The polarization ratio, $\sigma^\circ_{hh} / \sigma^\circ_{vv}$, is 3 - 5 dB in April and 2 - 8 dB in July. This is primarily a consequence of the multiple specular scattering by the trunks and the ground giving rise to a dihedral-like corner reflector effect. For the coniferous forest of Stand G, the predicted backscatter resulting from various scattering mechanisms is plotted versus angle of incidence in Figure 18. For both polarizations, σ° is shown to be dominated by the ground / trunk interaction mechanism. Direct backscatter from the crown layer is of secondary importance for σ°_{vv} and σ°_{hh}. For σ°_{hh}, the contributions from the crown layer and the crown / ground interaction mechanisms are roughly equivalent.

Similar to Stand G, the net backscatter from the northern hardwoods forest of Stand O is found to be dominated by the contribution from the ground / trunk interaction mechanism. Figure 19 shows contributions from direct scattering from the crown and crown / ground interactions to be of secondary significance to net σ°_{hh}. However, unlike Stand G, the net backscatter from the deciduous forest of Stand O is shown (in Figure 15) to change considerably from April to July; $\sigma^\circ_{April} > \sigma^\circ_{July}$ for all linear polarization. The contributions to σ°_{hh} of the various scattering mechanisms are shown in Figure 19 for both April and July. The decrease in σ° for the mid-summer conditions can be attributed to increases in foliar biomass and higher dielectric losses in the other crown layer constituents (large and small branches). These factors lead to much lower transmissivity through the crown layer during the July period. τ decreases from 0.5 in April to 0.4 in July at $\theta = 45^\circ$. The increased attenuation by the crown layer in July leads to a reduction in the contribution of the ground / trunk interaction mechanism (among others). The backscattering behaviors of the deciduous maple forests in Stands Q and T are similar in many respects to those discussed for Stand O.

Figure 18. Components of net P-band backscatter predicted by MIMICS for Stand G for (a) HH polarization and (b) VV polarization.

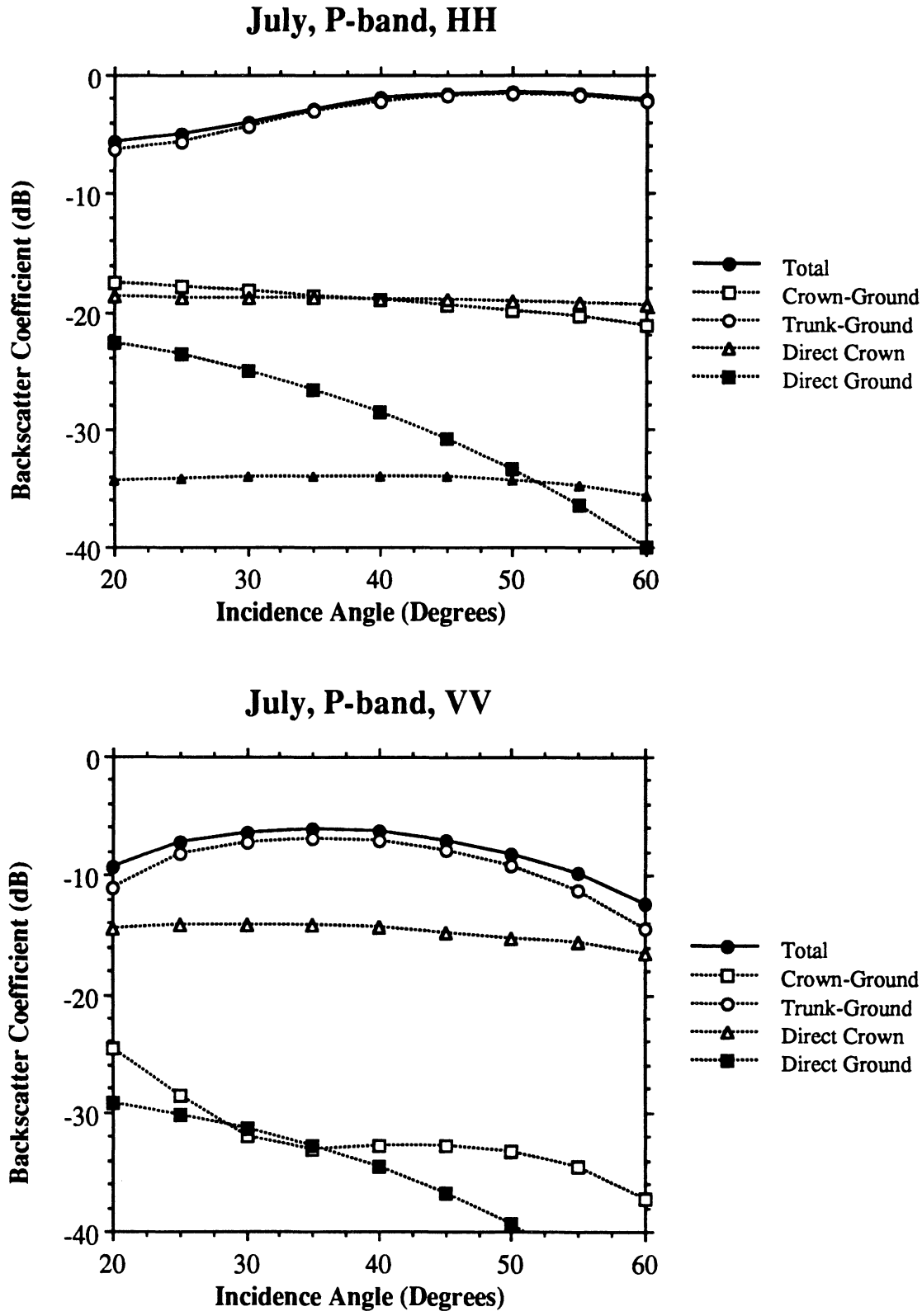

Figure 19. Components of net P-band backscatter predicted by MIMICS for Stand O at HH polarization for (a) April and (b) July.

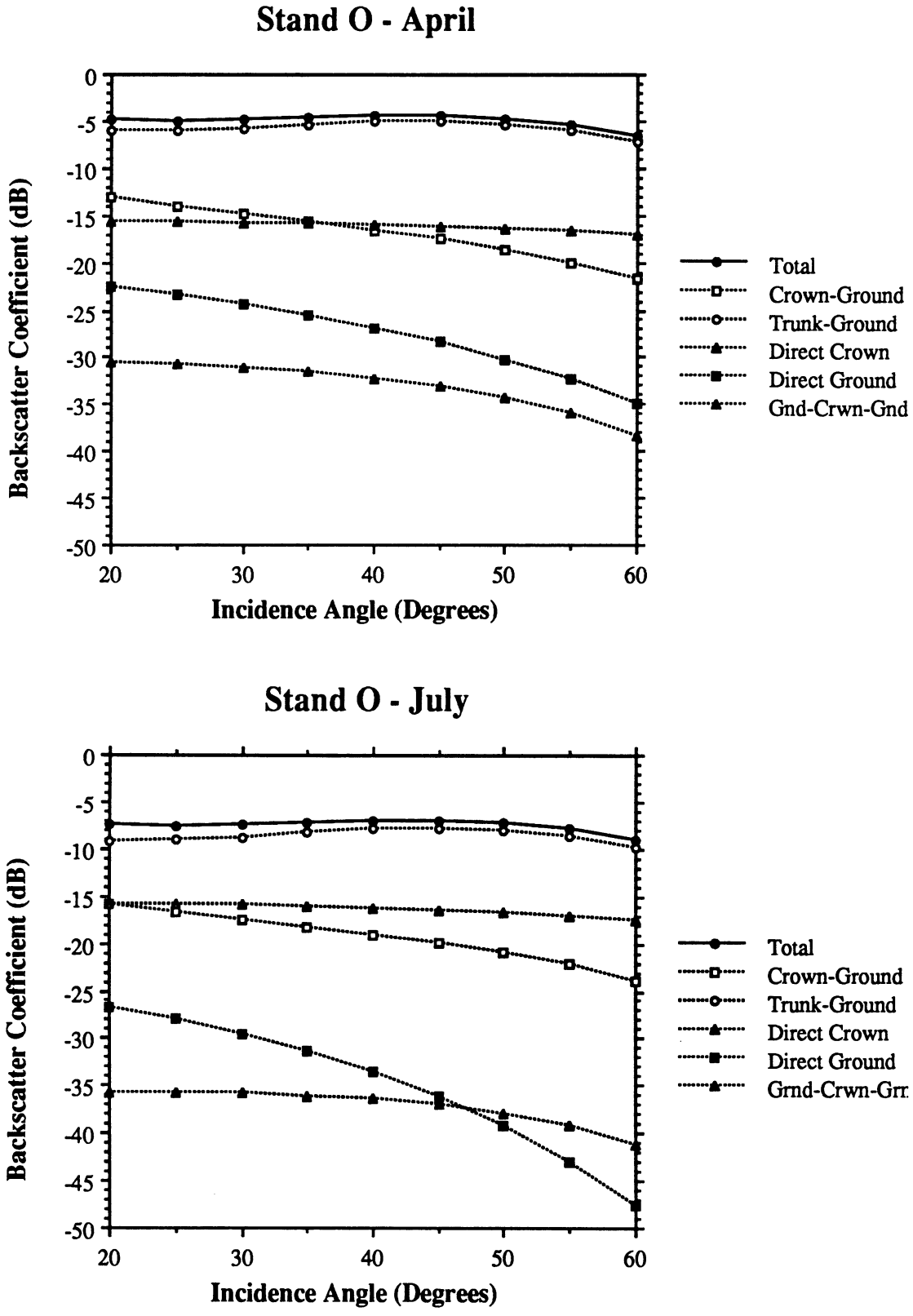

4.0 Conclusions

At P-band (440 MHz), the MIMICS model predicts that transmissivity and backscatter from forest stands can vary markedly both as functions of sensor parameters such as polarization and angle of incidence and as functions of forest architecture and dielectric properties. In the absence of freezing the vegetation canopy (such as might be found in the middle of winter), the dielectric properties of the canopy change somewhat (particularly an increase in the dielectric loss from April to July), but not dramatically. These dielectric changes, combined with increases in the summertime foliar mass of deciduous trees, lead to greater attenuation by the crown layer and a consequent decrease in expected σ° during mid-summer for deciduous forests. The magnitude of this decrease depends upon the specie composition of the forest stand. The MIMICS simulations show that total transmissivity τ is always greater for H polarization. This is primarily determined by the properties of the trunk layer. The near-vertical distribution of trunks couples strongly with V polarized propagating waves.

At P-band, the model predicts that net σ° is dominated by backscatter from the dihedral-like, ground / trunk interaction mechanism for both like polarizations. Backscattering mechanisms involving the crown layer are shown to be of secondary importance at this frequency. The backscattering contribution arising from the ground / trunk interaction mechanism will arrive at the radar contemporaneously with other mechanisms at the same range such as direct backscatter from the ground and backscatter from point targets on the ground surface. Hence, this contribution can be expected to produce significant background clutter which can be difficult to reject using broadband ranging techniques. It is significant to note that the magnitude of the ground / trunk interaction term is greatly reduced for VV and HV polarization.

A summary of the one-way extinction coefficients and radar backscattering coefficients predicted by MIMICS for the various forest stands is given in Table 18 for 440 MHz and a 45° angle of incidence. One-way extinction coefficient κ_e (dB/m) is transmissivity normalized by path length through the medium; $\kappa_e=(10\cos\theta\log\tau)/d$, where d is the layer thickness. Backscattering coefficient σ° is expressed as both the net backscatter and as the sum of those ground-related scattering mechanisms which would arrive simultaneously with a point target located on the ground.

The one-way transmission loss $L= -\kappa_e$. Since most of the crown layer constituent classes of branches and leaves are uniformly distributed, L_{crown} is shown to be independent of the angle of incidence in Figure 20. In contrast, the trunk layer is comprised of an array of near-vertical cylinders. Hence, L_{trunk} is found to vary with angle of incidence as shown in Figure 21. L_{trunk} always increases with angle of incidence.

In Table 18, κ_e of the crown layer is shown to vary between -0.1 to -0.46 dB/m depending upon forest type and observation date. $\kappa_{e\,crown}$ is greater for the deciduous forests than for the coniferous forest on any given date. This is primarily a result of the larger sizes of branches in the deciduous species. For the deciduous forests, $\kappa_{e\,crown}$ is greatest in July. One-way extinction by the trunk layer, $\kappa_{e\,trunk}$, is also found to vary as a function of forest type and observation date. $\kappa_{e\,trunk}$ is least for the coniferous forest (Stand G). The transmission losses through the trunk layer show seasonal variations for Stands Q and T, but are found to be nearly time constant for the more mature stands (Stands G and O).

For P-band at 45° incidence angle, Table 18 shows net backscatter σ° to be highly dependent upon forest type for like polarizations. σ°_{hv} is found to be relatively

Table 18 Summary of MIMICS simulation results.

Frequency = 440 MHz
Angle of incidence (relative to nadir) = 45°

Stand Designator / **Forest type**			**Stand G** Red pine	**Stand O** Northern hardwood	**Stand Q** Maple	**Stand T** Maple/Aspen
Radar backscatter (dB)						
HH pol.	April	Total	-2.70	-4.48	-4.64	-8.88
		Ground / trunk	-2.89	-5.04	-5.13	-10.11
		Sum of ground-related terms	-2.79	-4.79	-4.87	-9.47
	July	Total	-1.56	-6.99	-5.99	-12.26
		Ground / trunk	-1.72	-7.78	-6.92	-15.62
		Sum of ground-related terms	-1.64	-7.51	-6.51	-14.29
VV pol.	April	Total	-6.53	-8.45	-8.35	-10.29
		Ground / trunk	-6.84	-9.37	-9.06	-11.33
		Sum of ground-related terms	-6.76	-9.28	-8.93	-11.14
	July	Total	-7.00	-12.49	-10.74	-16.42
		Ground / trunk	-7.83	-14.98	-12.65	-19.25
		Sum of ground-related terms	-7.81	-14.83	-12.50	-18.95
HV pol.	April	Total	-19.92	-18.92	-17.89	-18.82
		Ground / trunk	-22.36	-23.84	-20.45	-21.51
		Sum of ground-related terms	-21.75	-22.56	-19.64	-20.70
	July	Total	-19.49	-20.27	-18.44	-25.28
		Ground / trunk	-21.55	-26.68	-23.70	-26.97
		Sum of ground-related terms	-21.23	-25.88	-22.18	-25.34
Path length		Crown layer	12.02	10.47	12.30	9.19
		Trunk layer	35.21	24.61	26.16	16.26
One-way extinction (dB/m)						
H pol.	April	Total	-0.098	-0.165	-0.117	-0.209
		Crown	-0.202	-0.284	-0.143	-0.231
		Trunk	-0.029	-0.044	-0.050	-0.078
	July	Total	-0.065	-0.203	-0.133	-0.324
		Crown	-0.108	-0.374	-0.196	-0.469
		Trunk	-0.029	-0.044	-0.041	-0.059
V pol.	April	Total	-0.129	-0.202	-0.176	-0.296
		Crown	-0.203	-0.279	-0.140	-0.227
		Trunk	-0.060	-0.083	-0.110	-0.168
	July	Total	-0.095	-0.240	-0.192	-0.402
		Crown	-0.108	-0.368	-0.194	-0.462
		Trunk	-0.058	-0.083	-0.101	-0.140

Figure 20. One-way loss through the forest crown layer calculated by MIMICS at P-band for (a) H- and (b) V-polarizations.

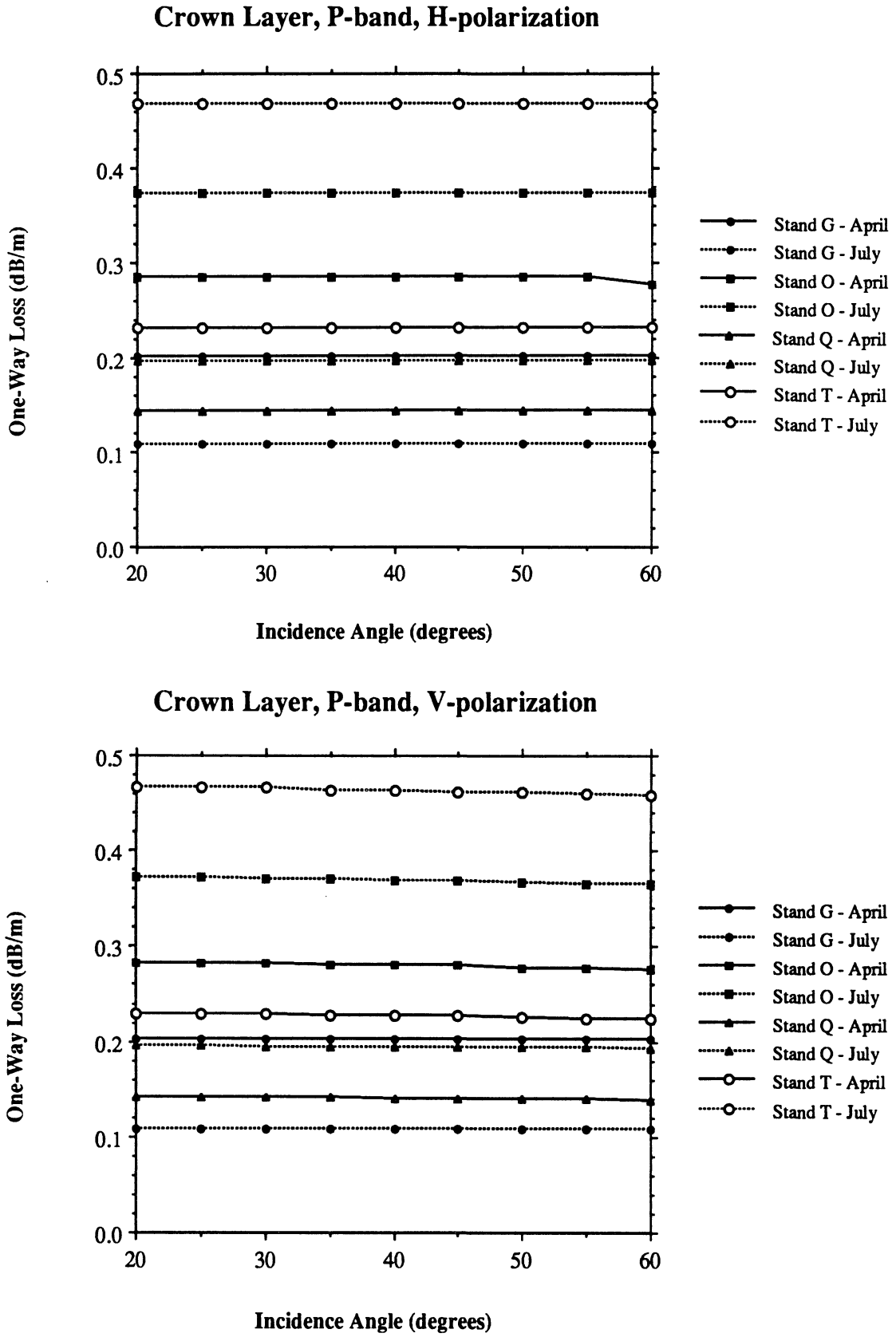

Figure 21. One-way loss through the forest trunk layer calculated by MIMICS at P-band for (a) H- and (b) V-polarizations.

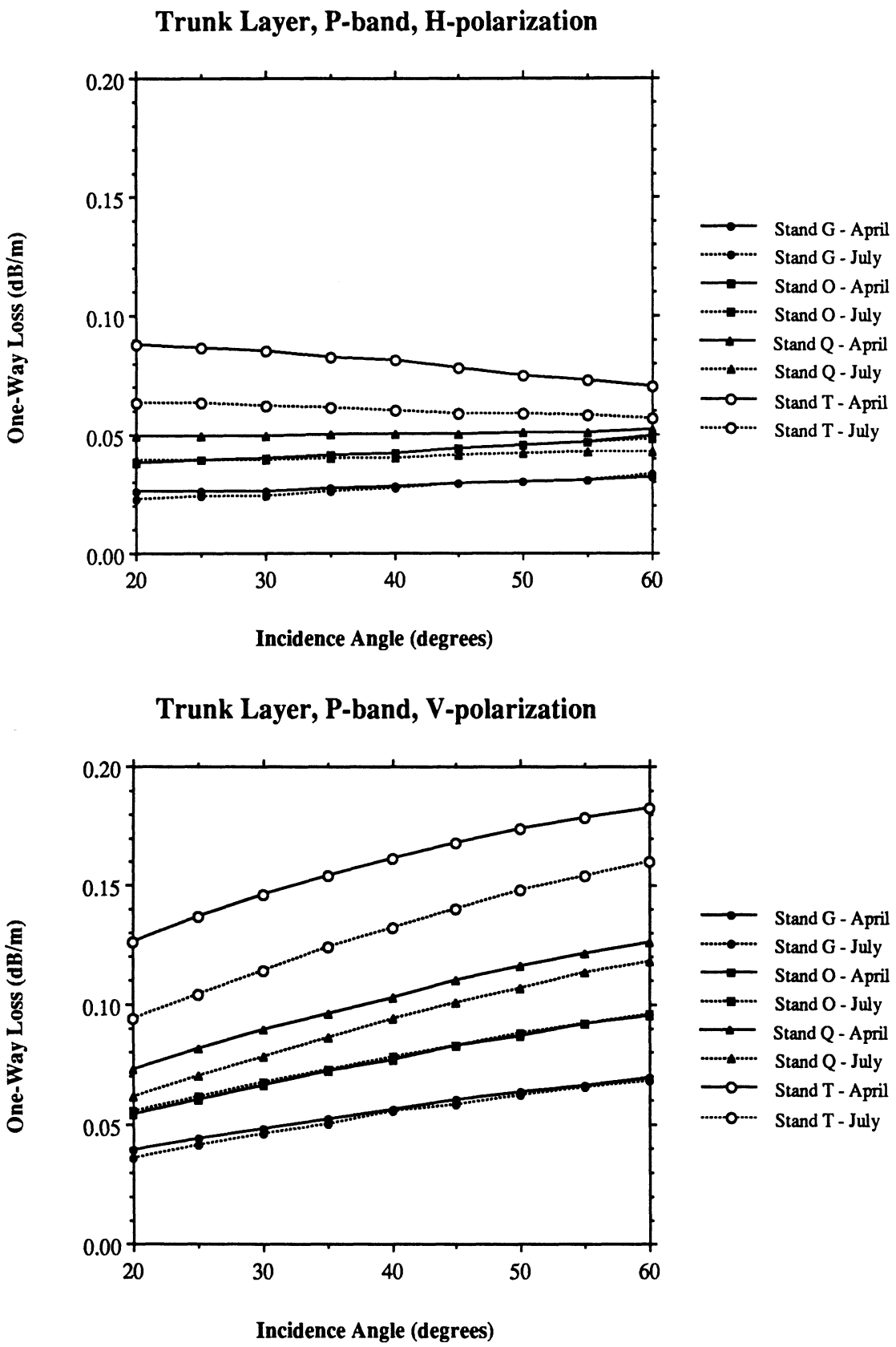

independent of forest type and observation date for the cases modeled; $\sigma^\circ_{hv} \approx$ -20 dB. For all of the modeled forest stands, σ°_{hh} is found to be dominated by ground related-scattering mechanism. These mechanisms include (in general order of significance): ground/trunk interactions, crown/ground interactions and direct scattering from the ground. When summed, these terms are found to account for more than 90% of σ°_{hh}. These same ground-related mechanisms are responsible for 60% to 95% of σ°_{vv}. Scattering by the crown layer is much more significant for σ°_{vv} but still of secondary import. For σ°_{hv}, the ground-related terms account for between 25% and 70% of net backscatter. In general, the ground-related scattering terms are most significant for coniferous forests; these forests tend to have a low density of large branches relative to wavelength.

Given the above, a P-band SAR with HH polarization will have the greatest ability to penetrate the crown and trunk layers of the forest canopy. However, HH polarization will also be most sensitive to forest clutter most of which is caused by scattering mechanisms which will be contemporaneous with direct backscatter from the surface beneath the forest. To the extent that point targets of interest are located at this range, this means that HH polarization can yield the lowest signal to noise ratio for point target detection even for a wide-band system using ranging techniques. VV and HV polarized SAR can be expected to overcome some of these obstacles since a far greater percentage of the net clutter return from the forest is shown to come from the crown layer which could be range-gated. For VV polarization, the backscatter from ground-related terms is found to be on the order of 4 dB to 7 dB less that this clutter source for HH polarization. Ground-related forest clutter is found to be lowest for HV polarization; 18 dB to 20 dB less than for HH polarization. However, the drawback of VV and HV polarizations is the greater extinction by of the V polarized waves, and by the trunk layer in particular.

ACKNOWLEDGMENTS

This effort was made possible with support from SRI, International. The following persons contributed to various stages of the planning, data acquisition, editing and analyses presented herein: Dr. John Vesecky, John Brown, Ruben DeLaSierra, James Slawski, Nai-Yu Wang and Eric Wilcox.

REFERENCES

[1] Dobson, M. C., "Ultra-Wideband SAR Forest Experiment Near Raco Michigan: April 4 - 12, 1992," Technical Report TR-029312-1, The University of Michigan, Radiation Laboratory, Department of Electrical Engineering and Computer Science, Ann Arbor, Michigan, 1992.

[2] Ulaby, F. T., K. Sarabandi, K. McDonald, M. Whitt, and M. C. Dobson, "Michigan Microwave Canopy Scattering Model (MIMICS)," International Journal of Remote Sensing, Vol. 11, No. 7, pp. 1223-1253, July 1990.

[3] McDonald, K. C., M. C. Dobson, and F. T. Ulaby, "Using MIMICS to Model L-Band Multiangle and Multitemporal Backscatter for a Walnut Orchard", IEEE Transactions on Geoscience and Remote Sensing, Vol. 28, No. 4, pp. 477-491, July, 1990.

[4] McDonald, K. C., M. C. Dobson and F. T. Ulaby, "Modeling Multifrequency Diurnal Backscatter From a Walnut Orchard," IEEE Transactions Geoscience and Remote Sensing, Vol. 29, No. 6, pp. 852-863, November, 1991.

[5] Gower, S. T. and J. M. Norman, "Rapid estimation of leaf area index in conifer and broad-leaf plantations using the Li-Cor LAI-2000," Ecology, Vol. 72, No. 5, pp. 1896-1900, 1991.

[6] Welles, J. M. and J. M. Norman, "Instrument for Indirect Measurement of Canopy Architecture," Agronomy Journal, Vol. 83, No. 5, pp. 818-825, 1991.

[7] Wilcox, E. and C. Dobson, "Leaf Area Index Data for the Michigan Forest Test Sites (1990-1991)", Radiation Laboratory Technical Report 025761-1-T, Department of Electrical Engineering and Computer Science, The University of Michigan, Ann Arbor, Michigan, January 1992.

[8] Dobson, M. C., F. T. Ulaby, M. Hallikainen, and M. El-Rayes, "Microwave Dielectric Behavior of Wet Soil, Part II: Dielectric Mixing Models," IEEE Trans. Geoscience and Remote Sensing, Vol. GE-23, No. 1, pp. 35-46, 1985.

[9] Ulaby, F. T. and M. A. El-Rayes, "Microwave Dielectric Spectrum of Vegetation, Part II: Dual-Dispersion Model," IEEE Trans. Geoscience and Remote Sensing, Vol. GE-25, No. 5, pp. 550-557, 1987.

[10] El-Rayes, M. and F. T. Ulaby, ""Microwave Dielectric Spectrum of Vegetation, Part I: Experimental Observations," IEEE Trans. Geoscience and Remote Sensing, Vol. GE-25, No. 5, pp. 541-549, 1987.

[11] Ulaby, F. T., M. C. Dobson, and D. R. Brunfeldt, "Microwave Probe for In Situ Observations of Vegetation Dielectric", Proceedings of IEEE Instrumentation Measurement Technology Conference (IMTC/90), May 14-16, 1991, Atlanta, Georgia, sub. to Trans. IMT July, 1991.

[12] Dobson, M. C., F. T. Ulaby, T. LeToan, A. Beaudoin, and E. S. Kasischke, "Dependence of Radar Backscatter on Conifer Forest Biomass," IEEE Transactions Geoscience and Remote Sensing, Vol. 30, No. 2, pp. 412-415, March, 1992.

[13] Hallikainen, M., F. T. Ulaby, M. C. Dobson, M. A. El-Rayes, and L. K. Wu, "Microwave Dielectric Behavior of Wet Soil, Part I: Empirical Models and Experimental Observations," IEEE Trans. Geoscience and Remote Sensing, Vol. GE-23, No. 1, pp. 25-34, 1985.

[14] Ruck, G. T., D. E. Barrick, W. D. Stuart and C. K. Krichbaum, Radar Cross Section Handbook, vol. 1, New York: Plenum Press, 1970.

[15] Sarabandi, K., "Electromagnetic Scattering from Vegetation Canopies," Ph.D. dissertation, The University of Michigan, 1989.

[16] Tsang, L., J. A. Kong and R. T. Shin, Theory of Microwave Remote Sensing, New York: John Wiley and Sons, Wiley-Interscience, 1985, pp. 160-162.

[17] Senior, T. B. A., K. Sarabandi and F. T. Ulaby, "Measuring and Modeling the Backscattering Cross Section of a Leaf," Radio Science, Vol. 22, No. 6, pp. 1109 - 1116, 1987.

[18] Tiuri, M. E., A. H. Sihvola, e. G. Nyfors and M. T. Hallikainen, " The Complex Dielectric Constant of Snow at Microwave Frequencies, "IEEE Jour. of Oceanic Engineering," Vol. OE-9, No. 5, pp. 377-382, Dec. 1984.